

Antihydrogen, probed with classical polarization dependent wavelength (PDW) shifts in the Lyman series, proves QFT inconsistent on antimatter

G. Van Hooydonk, Ghent University, Faculty of Sciences, Krijgslaan 281, B-9000 Ghent, Belgium

Abstract. Bound state QED uses the Sommerfeld-Dirac double square root equation to obtain quartics (Mexican hat or double well curves), which can give away left-right symmetry or chiral behavior for particle systems as in the SM. We now show that errors of Bohr 2D fermion theory are classical H polarization dependent wavelength (PDW) shifts. The observed H line spectrum exhibits a quartic with critical n-values for phase $\frac{1}{2}\pi$ (90°) and π (180°): phase $\frac{1}{2}\pi$ refers to circular H polarization (chiral behavior), phase π to linear H polarization and inversion on the Coulomb field axis. These signatures probe H polarization with 2 natural, mutually exclusive hydrogen quantum states ± 1 , i.e. H and \underline{H} . The \underline{H} signatures are consistent with polarization angles or phases, hidden in de Broglie's standing wave equation, which derives from Compton's early experiments with sinusoidal wavelength shifts. We refute the widely spread ban on natural \underline{H} and prove why QED, a quartic generating quantum field theory, classifies as inconsistent on neutral antimatter.

Pacs:

Introduction

The widely accepted ban on natural \underline{H} , proclaimed by theorists, led experimentalists to measure interval 1S-2S for artificially produced \underline{H} . Yet, we found unambiguous spectral signatures for \underline{H} in available H line and H₂ band spectra [1-5]. This \underline{H} -controversy could be settled once and for all with an ab initio H polarization theory but no such theory exists. This evident failure of theory can never mean that \underline{H} does not exist or that a ban on \underline{H} is legitimate. On the contrary, since \underline{H} is field-inverted H by definition, polarization dependent wavelength (PDW) shifts can interfere. We prove that errors of Bohr H theory are classical sinusoidal polarization dependent (PDW) shifts, leading to spectral signatures for \underline{H} [1-3]. A Bohr-type H polarization theory accounts for PDW shifts (\underline{H} -signatures) and leads to H boson behavior. With its ban on \underline{H} , QFT proves inconsistent neutral antimatter. This mistake finds its origin (i) in wrong interpretations of work by Sommerfeld and Kratzer and by Compton and de Broglie, all published around 1920, and (ii) of the Lamb-shift, exposed in 1947.

Generic sinusoidal appearance of polarization

Polarization of light, known for centuries, is a natural phenomenon, understood with a variable phase θ between 2 sinusoidal fields $a_0\cos\varphi+b_0\cos(\varphi+\theta)$. A 3D Poincaré sphere polarization model uses poles ± 1 and an equator to account for left-right or chiral properties of radiation: Cartesian frames for poles $+x$ and $-x$ are the mutually exclusive pair (left- and right-handed) $+x,+y,+z$ and $-x,+y,+z$ in vector calculus. Any H theory based upon a constant phase like Bohr's orthogonal phase of 90° must always fail on H polarization, which requires fields out of phase instead of fields in phase.

Polarization of matter and its chirality prove difficult, although observing polarization must be rather straightforward with its sinusoidal dependence on phase θ , a fractional angle absolutely confined to domain $0 \leq \theta \leq 2\pi$. Properly scaled sinusoidal effects are easily retraceable, whatever their magnitude. A dimension-less cosine law for a numerical field f consisting of 2 sub-fields

$$f(\theta) = \pm \sqrt{1 + (a/b)^2 - 2(a/b)\cos\theta} \approx \pm [1 - (a/b)\cos\theta \dots] \quad (1a)$$

(square bracket version valid for $b \gg a$), is a convenient basis to get at polarization in a Poincaré sphere. The square root in (1a) gives a tilted polarization ellipse for $b \neq a$ but returns an orthogonal system for $\theta = 90^\circ$ or $\frac{1}{2}\pi$ (a circle for $a = b$). With $b \gg a$ like in X-ray experiments for non-resonant interactions, (1a) gives sinusoidal fluctuations in function of phase θ , as observed by Compton¹ a long time ago [6]. Writing (1a) as $[1 - f(\theta)] / (a/b) \approx \cos\theta$ gives a cosine with generic asymptotes ± 1 . For the electron-proton Coulomb bond in composite H, numerical field (1a) has two variants

$$f(\theta) = \pm 1 / \sqrt{1 + (r_p/r_e)^2 - 2(r_p/r_e)\cos\theta} \approx \pm [1 + (r_p/r_e)\cos\theta \dots] \quad (1b)$$

$$f(\theta) = \pm 1 / \sqrt{1 + (m_e/m_p)^2 - 2(m_e/m_p)\cos\theta} \approx \pm [1 + (m_e/m_p)\cos\theta \dots] \quad (1c)$$

Strictly spoken, (1b) is a pair of conjugated unit charges short and (1c) is deceptive on mass as a scalar². Both variants are valid with internal field equations $m_e r_e = m_p r_p$ or $m_e/m_p = r_p/r_e$, the classical equilibrium conditions for bound states. Despite their gravitational basis, these are badly needed, even in quantum theories, to fix the origin of the reference frame for composite H, without which the basic equations for H and its complementary sub-particles cannot be formulated properly.

Polarization field problems are not solved with STR with orthogonal field $f(90^\circ) = \pm \sqrt{1 + (a/b)^2}$.

Although (1a) belongs to the classical 19th century Stokes-Maxwell-Poincaré view on polarization³, bound state QED uses a Dirac-field approach, inspired by Einstein's orthogonal STR equation

$$f(\alpha/n) = 1 / \sqrt{1 + (\alpha/n)^2} = 1 - \frac{1}{2}(\alpha/n)^2 + \frac{3}{8}(\alpha/n)^4 - \dots \quad (1d)$$

absolutely incompatible with (1a) needed for polarization, due to its lack of sinusoidals. How STR field (1d) had to be modified for H bound state QED is shown below. For full resonance of $h\nu$ (photons, boson symmetry and polarization) and H energies $E_1 - E_2$ (2 fermions) to be possible with

$$h\nu = E_1 - E_2 \quad (1e)$$

atom H must be credited with boson symmetry. Since Bohr's H is of fermion type, solutions based upon (1a)-(1c) for H, involving oscillations typical for boson behavior, must be envisaged. Compton's results led to de Broglie's the standing wave equation as a condition for resonance (1e) to occur

$$2\pi r = k\lambda \quad (1f)$$

which, in turn, led to non-relativistic Schrödinger wave mechanics and relativistic QFTs. In terms of field effects (1a-d), resonance condition (1f) hides a numerical quantized field ratio

$$r/\lambda = k/2\pi \quad (1g)$$

suggesting that de Broglie's quantum number k is competitive with phase θ with maximum 2π .

¹ which makes Compton polarimetry important for elementary particle physics [7].

² Reduced mass with complementary sub-masses $m_H = m_e + m_p = m_e + (m_H - m_e)$ is not a scalar (see below).

³ later on complemented with Jones [8] and Mueller matrices [9]

For polarization, this has drastic consequences, since rewriting de Broglie's relation (1g) as

$$r/(\frac{1}{2}\lambda) = k/\pi \text{ and } r/(\frac{1}{4}\lambda) = k/\frac{1}{2}\pi \quad (1h)$$

gives a half wavelength plate with k equal to 180° or π , known to transform left- in right-handed radiation, while a quarter wavelength plate acts accordingly in terms of classical optics.

Bohr-type H polarization

Without specifying sub-fields or ratio a/b , using (1a) in Bohr bound state $(1-1/n^2)$ theory gives

$$\begin{aligned} h\nu = hc/\lambda = [1/f(\theta_0) - 1/(n^2 f(\theta))] \sim &+ \{ [1 + (a/b)\cos\theta_0] - (1/n^2)[1 + (a/b)\cos\theta \dots] \} \\ &\sim + (1-1/n^2) + (a/b)(\cos\theta_0 - \cos\theta/n^2) + \dots \end{aligned} \quad (2a)$$

for resonance to occur, with θ_0 constant. Equation (2a) returns Bohr term $(1-1/n^2)$ but adds sinusoidal polarization dependent wavelength (PDW) shifts Δ_p of order a/b . H PDW shifts, exposed with (2a), cannot but be interpreted as errors Δ_p of Bohr theory. Analytically, H PDW shifts obey

$$\Delta_p \sim [(1-1/n^2) + (a/b)(\cos\theta_0 - \cos\theta/n^2) + \dots] - (1-1/n^2) = (a/b)(\cos\theta_0 - \cos\theta/n^2) + \dots \quad (2b)$$

$$\Delta'_p \sim [(1-1/n^2) - (a/b)\cos\theta/n^2 + \dots] - (1-1/n^2) = -(a/b)\cos\theta/n^2 + \dots \quad (2c)$$

with $\Delta'_p = \Delta_p - (a/b)\cos\theta_0$, and apply for terms $(1-1/n^2)$ and energies $-1/n^2$, without affecting the sinusoidal appearance. With $1-\cos\theta = 2\sin^2(\frac{1}{2}\theta)$ and/or $1+\cos\theta = 2\cos^2(\frac{1}{2}\theta)$ for (2), non-sinusoidal effects $(a/b)/n^2$ in (2) can appear for H PDW shifts in Bohr-like H polarization theory (2a).

H PDW shifts, if any, should vary as $\cos\theta/n^2$. Rewriting (2c) as $(b/a)n^2\Delta'_p \sim \cos\theta$ gives generic sinusoidal behavior. Generic polarization with phase θ is illustrated in Fig. 1a, using a cosine with asymptotes ± 1 . Maximum phase 2π , divided in 20 parts $2\pi/20 = \pi/10$ is centered as $-\pi, +\pi$ and scaled to $-1, +1$. The fractional angle or phase varies with $2(n-1)\pi/20$ when n goes from 1 to 21, which makes x- and y-axis commensurate. Fig. 1a for polarization needs some comments.

(i) Fig.1a exposes the generic relation between phase θ and handedness: linear polarization for $\cos\theta=0$ (0° , parallel fields) or π (180° , antiparallel fields, with a field inversion), circular⁴ polarization for poles $+1$ and -1 , $\cos\theta = \frac{1}{2}\pi$ (90° , say right handed, orthogonal equal fields) or $-\frac{1}{2}\pi$ (-90° or 270° , say left-handed, orthogonal equal fields) and elliptical polarization in between⁵. The phase needed to switch from left- to right-handed polarization is exactly 180° , implicit in de Broglie's relation (1h).

(ii) Sinusoidal pattern in Fig. 1a shows with laser signals in optical fibers [10-12]. When bit-compression is high (order G-THz), signals are affected by polarization. Distortions in data transmitted between Alice and Bob, due to formerly unknown polarization dependent losses [10-12], led to practical problems⁶. With Fig. 1a, observed photon (boson) polarization relates with entanglement, quantum computing, Bell-inequalities and EPR-tests using polarization of photons or neutral particles, like the kaon [10-11].

⁴ which also requires 2orthogonal fields of equal magnitude.

⁵ Complementary sine can be used for polar shifts, since polar and equatorial axes are assigned by convention.

⁶ Restoring signal distortions by PMD losses or PDW shifts relies on fiber Bragg or chiral gratings [12].

(iii) In material system H, sinusoidal effects (2c) diminish with $1/n^2$. Since the smaller the size, the larger the density (compression), this situation compares with bit-density effects for photon polarization. For $1/n^2$ H theory, this gives compacted attenuated sinusoidals like in Fig. 1b-c, where $\cos(\pi n/10)/n$ and $\sin(\pi n/10)/n$ (Fig. 1b) and $\cos(\pi n/10)/n^2$ and $\sin(\pi n/10)/n^2$ (Fig. 1c) are plotted versus $1/n$. In this phenomenological H polarization model, distorted sinusoidals in Fig. 1b-c can be extrapolated to the left (expansion, low density) and even beyond $n=\infty$ or $1/n=0$, where H no longer exists (horizon problem). Extrapolation to the right (compression, high density) goes beyond ground state $n=1$, a strange consequence, discussed below. Attenuated, distorted sinusoidals in Fig. 1b-c only seem different from those in Fig. 1a but are related by Bohr packing factors $1/n$ (odd) or $1/n^2$ (even).

(iv) For resonant interactions between radiation and matter, all details in Fig. 1a for boson polarization will have to match exactly all those of fermion system H for resonance to be possible with (1e). If radiation showed left-right behavior, H must show this behavior too when its spectrum is measurable. Simplest atom H is a prototype for resonant interactions and cannot be an exception. On the contrary, the H spectrum is the simplest tool imaginable to get at polarization for the so-called electron-proton Coulomb bond, its sinusoidal effects (1a-c) and, eventually, its boson (photon) behavior.

(v) Observed line profiles (including wavelength shifts), are affected by an atom's environment. Field effects can be eliminated by extrapolation to zero field (Zeeman, Stark). Interatomic interactions of a resonating atom with identical or foreign neighbors also affect line profiles. If sinusoidal [13], these can be eliminated with extrapolation towards the difficult single atom case. Even so, their influence can be minimized using field effects for a couple of closely spaced lines, extrapolated to zero-field. This reliable procedure was used for 2 nearly degenerate lines (see the Lamb-shifts below).

(vi) With sinusoidal environmental effects accounted for, information on intra-atomic polarization is assessable. This brings in \underline{H} , forbidden in nature, because of charge anti-symmetry and annihilation in the Dirac-sense, although \underline{H} is also electrically neutral. Theorists argue that \underline{H} , the right- (left-) handed version of left- (right-) handed H, is forbidden, although the two are just the natural, mutually exclusive quantum states ± 1 , H and \underline{H} , possible for a polarized H atom. The 2 atom states correspond with the 2 quantum states ± 1 for bosons (radiation) or even with the generic cosine asymptotes ± 1 as depicted in Fig. 1a. Instead of vetoing \underline{H} , one should at least have admitted a long time ago that both states H and \underline{H} are theoretically possible and allowed for natural, neutral, stable composite Coulomb atom hydrogen, when polarized. If 2 quantum states ± 1 for hydrogen are both stable, they must be described with an inversion along the Coulomb field axis (bipolar view), i.e. with attraction of 2 unit charges $-e_1e_2$, say $+1$, inverted to $-e_2e_1$, say -1 . These are linear sum- and difference-states in (1a), i.e. $1 \pm m_e/m_p$ in (1c) and $1 \pm r_p/r_e$ in (1b). A permutation on an axis is a rotation exactly by 180° or π for one of 2 complementary parts in H. For (2a) to give (a+b), $\cos\theta = -1$ or $\theta = \pi$ is required, while for difference (a-b) $\cos\theta = +1$ or $\theta = 0$, vector sum and difference having different orientations in space. For full resonance between H and radiation to be possible with (1e), H should be credited with some boson behavior.

(vii) If polarized H-states have always been observed from the 19th century on, these are in full resonance with radiation in the absence of (strong) external fields. If so, only the H spectrum can decide on H polarization, on boson behavior and on the fate of H. Theoretically possible, plausible state H can never be forbidden, before the H spectrum is tested, without prejudice or bias, for generic H polarization effects like those in Fig. 1a.

Testing the H spectrum for sinusoidal effects using planar Bohr R/n^2 fermion theory

The advantage of simple Bohr $1/n^2$ theory for fermions is that it is exclusively planar 2D (rotational freedom), without the preferential direction, needed for polarization. Bohr's circular model uses a constant unit field $1/\sqrt{(\cos^2\varphi+\sin^2\varphi)}=1/\sqrt{(\cos^2\varphi+1-\cos^2\varphi)}=1/\sqrt{(1-\sin^2\varphi+\sin^2\varphi)}=1$ with constant phase 90° between sine and cosine, which means that it is a constant Rydberg R theory $-R/n^2$. A variable phase θ as in (1a) creates problems for circular orbits, since $1/\sqrt{[\cos^2\varphi+1-\cos^2(\varphi+\theta)]}$ is equal to 1 only for $\theta=0^\circ$. Strange as it may seem, these difficult theoretical problems with polarization, caused by a variable not constant phase θ , make Bohr $-R/n^2$ fermion theory a unique tool to quantify H behavior beyond 2D, i.e. when polarization with variable phase would show as in (2a) [2]. Theoretical level energies (in cm^{-1})

$$-E_{n(2D)} = R/n_B^2 \text{ cm}^{-1} \text{ or } 1/n_B = \pm\sqrt{(-E_{n(2D)}/R)} \quad (3)$$

with Bohr's n_B an integer and constant R , are easily confronted with observed energies $E_{n(\text{exp})}$, denoted in a similar way with effective or experimentally observed numbers n_{exp} or

$$-E_{n(\text{exp})} = R/n_{\text{exp}}^2 \text{ cm}^{-1} \text{ or } 1/n_{\text{exp}} = \pm\sqrt{(-E_{n(\text{exp})}/R)} \quad (4a)$$

This gives simple numerical relations

$$E_{n(2D)}/E_{n(\text{exp})} = (n_{\text{exp}}/n_B)^2 \text{ or } \pm(n_{\text{exp}}/n_B) = \pm\sqrt{(E_{n(2D)}/E_{n(\text{exp})})} \quad (4b)$$

Using Rydbergs R_B and R_{exp} in cm^{-1} with integers n_B in either case leads to an alternative test

$$R_{\text{exp}} = R_H(n) = (E_{n(\text{exp})}/E_{n(2D)})R_B = E_{n(\text{exp})}n_B^2 \text{ cm}^{-1} \quad (4c)$$

based running Rydbergs $R_H(n)$ instead of constant R [2]. Differences Δ_n between n_B in (3) and n_{exp} in (4), not necessarily an integer if sinusoidal (2) is in operation, obey dimension-less numerical relations

$$\Delta_n = 1/n_B - 1/n_{\text{exp}} = (n_{\text{exp}} - n_B)/n_B n_{\text{exp}} = \pm[\sqrt{(-E_{n(2D)}/R)} - \sqrt{(-E_{n(\text{exp})}/R)}] \quad (5a)$$

$$\begin{aligned} \Delta_n' &= 1/n_B^2 - 1/n_{\text{exp}}^2 = (1/n_B - 1/n_{\text{exp}})(1/n_B + 1/n_{\text{exp}}) = (n_{\text{exp}}^2 - n_B^2)/n_B^2 n_{\text{exp}}^2 \\ &= [(-E_{n(2D)}/R) - (-E_{n(\text{exp})}/R)] \end{aligned} \quad (5b)$$

implying that $\Delta_n'/\Delta_n \approx 2/n$. R_{exp} in cm^{-1} in (4c) as well as numbers Δ in (5a-b) must all be of sinusoidal type, for H polarization (2a), H boson behavior and its 2 quantum states H and H to make sense.

At the time, it was expected that results for the H spectrum using Einstein's STR-field (1d)

$$\Delta(\text{STR}) = E_{n(2D)} - \mu c^2 [1/\sqrt{(1+(\alpha/n)^2)} - 1] \quad (5c)$$

would be better than with constant R , the Bohr field. In reality and despite these high expectations, testing STR field (1d) with (5c) proves this orthogonal field is much less precise than naïve Bohr

theory, as we show below. This summarizes the status of H bound state theories around the 1920s as well as the theoretical possibilities available at the time to test Bohr theory beyond its 2D limit.

Observed sinusoidal effects in the H line spectrum and Bohr-type polarization theory

The H Lyman series $ns_{1/2}$ and $np_{1/2}$ are available for testing with Kelly's observed terms (errors of $0,0001 \text{ cm}^{-1}$) [14] or with Erickson's energies, according to QED calculations (errors $0,0000001 \text{ cm}^{-1}$) [15]. R , needed in (5), is $109678,7737 \text{ cm}^{-1}$ in [14] and $109678,773704 \text{ cm}^{-1}$ in [15]. Data are in Table 1. Since the consistency of H bound state QED is at stake, we use QED data [15], although Kelly data [14] give similar results. The 4th order fit of the 2 series [15] with $1/n$ gives respectively

$$-E_{ns} = -4,365136/n^4 + 5,552171/n^3 + 109677,586807/n^2 - 0,000143/n + 0,000005 \text{ cm}^{-1} \quad (5d)$$

$$-E_{np} = -4,377663/n^4 + 5,842957/n^3 + 109677,585445/n^2 - 0,000008/n \text{ cm}^{-1} \quad (5e)$$

The fits return energies with average errors of only 7,8 kHz and 0,8 kHz respectively. Kelly terms T_{ns} [14] are compatible with (5d). As an example, fitting his observed ns-terms [14] gives

$$T_{ns} = 4,365740/n^4 - 5,553058/n^3 - 109677,586558/n^2 + 0,000133/n + 109678,773744 \text{ cm}^{-1} \quad (5f)$$

which matches (5d) when comparing coefficients.

Neglecting the smaller terms in (5d) and using (4c), observed running Rydbergs for ns obey

$$R_{exp} = -E_{ns}n^2 = -4,365136/n^2 + 5,552171/n + 109677,586807 \text{ cm}^{-1} \quad (5g)$$

Tests (4c) and (5) on H symmetries or on the constancy of R lead to straightforward conclusions.

(i) The parabolic result for running Rydbergs (4c) in Fig. 2a immediately falsifies Bohr's constant Rydberg thesis R/n^2 for a fermion model as it reproduces (5g). The similar result in Fig. 1 of [2]⁷ is repeated here for (4c) with the harmonic Rydberg ($109679,35 \text{ cm}^{-1}$) included. This Rydberg is tangent to the complete series and can be considered constant in the spirit of the circular orbits of Bohr fermion 2D theory and phase 90° for sine and cosine. It touches the parabola at $n_0 = 1/2\pi$ [2] but deviates, in a sinusoidal manner, from this critical value⁸. The absence of a preferential direction in Bohr theory is visualized with horizontal lines, parallel to the x-axis in Fig. 2a, like the dashed line for $n=1$, the so-called H ground state at $R_1 = 109678,7737 \text{ cm}^{-1}$. The classical H anchor at the extreme in Fig. 2a is obtained by removing Bohr's attenuation factor $1/n^2$ using (4c). The observed result for R is strikingly similar with that with the cosine for generic polarization in Fig. 1a. Comparing curves, it is evident that the curves for H Rydbergs in Fig. 2a are of type $(1 - \cos\theta) = 2\sin^2(\theta/2)$. Its square root implies that observed H symmetries depend on $\sin(\theta/2)\sqrt{2}$, in agreement with polarization theory. These straightforward implications of Fig. 2a led us directly to H and justify the brief report of 2002 [2,4].

⁷ There is a typo in its Eqn. (1).

⁸ This angle of 90° remains constant in planar circular models but does not show explicitly, since complementary sine and cosine are used. At first sight, retrieving this angle with a spectrum seems a logical consequence of the reality of 2 orthogonal fields and circular orbits. Yet, finding out that this angle is no longer constant in a complete series but critical instead is a true signature for H polarization [2]. This relies on deviations from 90° instead of remaining constant.

(ii) Parabolic behavior of running Rydbergs in Fig. 2a points to sinusoidal behavior, since in first order $1-\cos\theta=1-(1-\frac{1}{2}\theta^2+\dots)\approx\frac{1}{2}\theta^2$. Since this suggests boson behavior, Fig. 2a shows that a boson-like H atom appears when Coulomb attraction sets in at $1/n=0$. It reaches its maximum at $n_0=\frac{1}{2}\pi$ upon compressing the 2 H fermions (electron and proton), and then gradually diminishes. In terms of H fermion-boson symmetries, the extreme marks a transition between different H symmetries, while only H fermion symmetry can be considered as constant in the full interval, pending the choice of the asymptote ± 1 to describe it. The choice of an asymptote, $+1$ or -1 , is purely conventional but can never mean that one of them does not exist – see sine and cosine--, which also puts question marks on a veto on H). The appearance of H boson symmetry is now understandable, since it is essential for full resonance between system H and radiation (a boson structure) to be possible by virtue of (1e).

(iii) More details on H behavior beyond 2D are exposed with the curves for differences (5a)-(5b), shown in Fig. 2b,c. These are extrapolated, since it is uncertain how restricted observable domain for H, i.e. $2\geq n\leq\infty$ or $\frac{1}{2}\leq 1/n\geq 0$, will comply with the full domain 2π for phase θ (see further below). Compacting effects, illustrated in Fig. 1b-c, are now clearly visible with the H spectrum. Attenuation by $1/n$ or $1/n^2$ must not distract from the sinusoidal character of Δ_n . In fact, the H spectrum shows that all perfectly sinusoidal curves for $1/n$ (5a) in Fig. 2b and for $1/n^2$ (5b) in Fig. 2c are consistent with parabola (5g) for R_{exp} , given in Fig. 2a and in Fig. 1 of [2].

Visual inspection of all Fig. 2 proves beyond any doubt that deviations from Bohr's 2D fermion model for H are sinusoidal, which confirms the existence of sinusoidal field fluctuations (2), needed for polarization to appear in natural neutral Coulomb system H. With Fig. 1 and 2, observation [14] as well as bound state QED theory [15] both point to sinusoidal Compton-like wavelength shifts (1) in H, which led to de Broglie' equation (1f) and generic polarization angles like (1h).

To prove that these are indeed H PDW shifts, conform Fig. 1a for the polarization of light, the phase correlation of Fig. 1a must be retraced identically in the H spectrum: phase $\pm\frac{1}{2}\pi$ for circular and phase 0 or π for linear H polarization are both required, as argued in [2-3]. With Fig. 1-2, our earlier, rather bold conclusions on the existence of natural H-states are fully justified [2].

However, the origin of pertinent H-signatures must be retraced in bound state QED. We remind that orthogonal STR field (1d) had to be modified drastically to account for the very same H-states in Fig. 2a-b. In fact, Fig. 2d shows the result of test (5c) for STR. Highly praised STR field (1d) is worse than Bohr's: it simply proves disastrous⁹. Repulsive term in $1/n^4$ creates errors, much larger than those of simple Bohr $-R/n^2$ theory, as shown in Fig. 2d. STR errors are 12 and 27 times larger than Bohr's for respectively np and ns (not shown). To undo the damage of the STR field, large attractive corrections of order $-5,84/n^3 \text{ cm}^{-1}$ for np and $-5,55/n^3 \text{ cm}^{-1}$ for ns were needed (see below). Fig. 2d is illustrative for the history of theoretical physics. Perhaps theorists were misled: they were preoccupied with the great errors of the H STR-field (upper 2 closely spaced curves in Fig. 2d), which could have made

⁹ This flagrant erratic behavior of STR for H (Fig. 2d) is never mentioned, it certainly was not in Einstein Year 2005 [1]

them overlook the small errors of Bohr theory, wherein harmonic and quartic behavior already shows (lower 2 curves in Fig. 2d). Even with moderate spectral accuracy, the large errors of STR were clearly visible, the smaller ones of Bohr theory far less (Fig. 2d).

How to remove these large STR errors had a great impact on theorists but may well have distracted their attention from the real problem: H polarization. It was probably not realized that Bohr theory is so reliable and powerful to disclose 3D effects beyond 2D, e.g. H polarization effects (Fig. 2d). This makes the history of these attractive corrections, so badly needed for erratic STR bound state H field theory (1d), quite remarkable.

Origin of Sommerfeld's double square root equation and quartics in bound state QED

Classical Coulomb and polarization models for composite H differ in that the first is planar (2D), due to a central field approximation, whereas the second points to out of plane effects with a bipolar view, essential to arrive at H polarization. Although Bohr's $1/n^2$ H 2D fermion theory is fairly accurate (parts in 10^7 for terms, 300 MHz), replacing it with its also highly praised 3D Schrödinger wave mechanical version proved unsatisfactory [1], as the accuracy was no better¹⁰: Schrödinger returned the very same energy levels of Bohr's $1/n^2$ theory, without any correction term added.

In the early 20th century and before Schrödinger, physicists like Sommerfeld, Kramers, Bohr... were all occupied with the discrepancies between $-R/n^2$ theory and experiment. Theoretical corrections, inspired by Einstein's (1d), led to even greater errors than with a naïve, constant Bohr field (see Fig. 2d) and caused a great dissatisfaction with highly praised STR theory amongst notorious relativists. Even with moderate accuracy, positive as well as negative deviations from a constant Rydberg hypothesis $-R/n^2$ suggested fluctuating deviations (see Fig. 2d). Sommerfeld's azimuthal quantum number $\ell=n-1$ and his 2D elliptical model, useful for classifying states, did not improve the accuracy either.

Unlike Schrödinger, Sommerfeld must have realized at a very early instance that only parabolic oscillatory behavior (e.g. tilted instead of planar ellipses) would account for remaining discrepancies and that, at the same time, only a large attractive term $-1/n^3$ would restore the damage by STR (see Fig. 2) of great concern for relativists and theoretical physicists.

Knowing this, Sommerfeld suggested his pupil Kratzer¹¹ to work on a numerical parabola [17]

¹⁰ Apparently, wave mechanical H does not improve $-R/n^2$ theory [1]. This procedure has angular dependencies *in phase* to get at resonance (and to remain soluble), instead of *out of phase* to get at polarization-states needed for full resonance.

¹¹ Rigden [16] does not mention that Kratzer was Sommerfeld's pupil. Kratzer's potential $V(r)=-e^2/r + b/r^2$ and $V(r_0)=-1/2e^2/r_0$ figures at length in Sommerfeld's famous monograph [18]. It is probably the most underestimated potential in physics and chemistry [19](see also Appendix). A molecular Kratzer potential is universal. It is superior to Morse's and accounts smoothly for lower order spectroscopic constants of 300 diatomics X_2 [19-20]. Kratzer's potential (6) refers to the 19th century ionic Coulomb X^+X^- , not to the covalent asymptote XX . This seems to favor old-fashioned classical Coulomb ionic bonding $-e^2/r$ but, in reality, it gives away atom-antiatom or XX bonding [1,20], although a ban on H implies a ban on HH and on HH -oscillations [21]. The conventional argument, often used, against XX bonding is that it contradicts mainstream physics and chemistry!

$$E_p \sim (1-n_0/n)^2 \quad (6)$$

where n_0 is a critical internal quantum number for H, missing in Bohr-Schrodinger theories. Although at the time, Kratzer's potential (6) was considered typical for oscillations between atoms in molecules¹² (see Appendix), Sommerfeld knew it would automatically improve the precision of a new theory, in which Bohr-Schrödinger $1/n^2$ term had to remain. His own quantum number $\ell=n-1$ and

$$\alpha=e^2/\hbar c = 1/137,035999\dots \quad (7)$$

his numerical field scale factor (the fine structure constant, first referred to in 1915), should be conserved too. The Sommerfeld-Kratzer connection is now easily understood. Sommerfeld's number $\ell=n-1$ is connected with Kratzer's potential (6): with $n_0=\ell$, (6) is degenerate with Bohr's $1/n^2=(1-\ell/n)^2=[1-(n-1)/n]^2=(1-1+1/n)^2=1/n^2$. But for $\ell=0$ (circular orbits), the effect of (6) with integer n would vanish identically. Even with constant n_0 , (6) gives results equivalent to Bohr's, for any intermediary asymptote (Rydberg), virtual or not, we would choose. Putting $R/n^2=A(1-n_0/n)^2$, always returns an exact numerical relation between a scaled asymptote $\sqrt{R/A}=n-n_0$, without loss of precision. The procedure (not shown) is easily verified with a plot of terms or levels versus n_0/n or versus $(n_0/n-1)$, with n_0 integer or not. The linear $1/n$ procedure is exemplified with (5a) and Fig. 2b. With this evidence in mind, Sommerfeld, a reputed convinced relativist, also knew too well that the Einstein-STR expansion for H on the basis (1d), used for (5c)

$$-E_n/\mu c^2=[1/f_{STR}(n)-1]=1/\sqrt{1+\alpha^2/n^2}-1=1-1/2\alpha^2/n^2+3/8\alpha^4/n^4-\dots-1=(-1/2\alpha^2/n^2)(1-3/4\alpha^2/n^2-\dots)(8)$$

can never give parabolic behavior of type (6). Term $+3/8\alpha^4/n^4$ in (8) may be small indeed and of the required magnitude, it remains exclusively repulsive. For H, it creates rather than solves problems for Bohr $1/n^2$ theory, as shown in Fig. 2d. Sommerfeld associated the more visible Kratzer parabola (6) with higher order attractive terms in an STR expansion, to arrive at terms of mixed type

$$E_p \sim (\alpha^4/n^2)(1-n_0/n)^2 \quad (9)$$

intimately connected also with his quantum number ℓ as shown above.

The challenge for Sommerfeld was that STR (8) had to be modified drastically, while he was forced to retain Bohr, Kratzer (6) and Einstein STR (8) theories as well as his own quantum number ℓ . To get agreement to a modified STR field and observation was now a matter of mathematical skills, just like those of Sommerfeld. Not surprisingly, these led him to a remarkable, ingenious double square root¹³ solution for H with reduced mass¹⁴ μ , i.e.

$$E_{n,j}=\mu c^2[f(n,j)-1]=\mu c^2 f(n,j)-\mu c^2 \quad (10)$$

$$f(n,j)=\left\{1+\alpha^2/\left[\sqrt{\left(j+\frac{1}{2}\right)^2-\alpha^2}+n-j-\frac{1}{2}\right]^2\right\}^{-1/2} \quad (11)$$

This new STR-like field factor $f(n,j)$ in (11), today textbook material and once considered as the latest

¹² Sommerfeld obviously made oscillations (bosons) interfere with rotations (fermions): this makes him the pioneer of supersymmetry (SUSY, MSSM), although, at the time, the fermion-boson symmetry concept was not used.

¹³ More than a century ago, Ramanujan, once at Trinity, found a connection between double square roots and quartics [22].

¹⁴ It is strange that (10) uses μ , although at $n=\infty$, an electron with mass m_e instead of μ is set free. There is no reason to use reduced mass in STR based (10), as remarked by Cagnac et al. with some irony [23]. They write that the only justification (sic)[used by Cagnac] to use reduced mass μ in (10) is that it makes this equation consistent with experiment [23] (see below).

real cornerstone of theoretical physics, is similar to $f_{\text{STR}}(n)$ in (1d) or (8) but different. Its validity, if confirmed by the H spectrum, would immediately flaw original Einstein STR equation (1d) or (8), as evident with Fig. 2d. Also, j is the total angular quantum number, with values $j = +\frac{1}{2}$ for $\ell=0$ and $j = \ell \pm \frac{1}{2}$ for $\ell \neq 0$, where $\ell=n-1$ is Sommerfeld's number. It is retrieved exactly in (10)-(11) for atom states obeying $j+\frac{1}{2}=1$, for which $n-j-\frac{1}{2}=n-(j+\frac{1}{2})=n-1=\ell$. Looking at Fig. 2d, these derivations place the famous double square root equation (10)-(11) of modern bound state QED in a different context: it was simply needed by Sommerfeld to fit his azimuthal quantum number and oscillatory (boson) behavior (6) into a very badly performing relativistic Bohr-Einstein (fermion) rotator (8) because of sinusoidal errors remaining for H with Bohr's planar $1/n^2$ theory¹⁵.

In fact, the difference between (10) and (8) may be subtle, the connection with ℓ and Kratzer's (6) is obvious. For $j+\frac{1}{2}=1$ with $\ell=0$ and $\ell=1$, terms between square brackets in (11) simplify as

$$\begin{aligned} \sqrt{[(j+\frac{1}{2})^2-\alpha^2]+n-j-\frac{1}{2}} &= \sqrt{(1-\alpha^2)+(n-1)} = \sqrt{(1-\alpha^2)+\ell} \\ &= (n-\frac{1}{2}\alpha^2)^2 \approx n^2 - n\alpha^2 = n^2(1-\alpha^2/n) \end{aligned} \quad (12)$$

$$f(n, j+\frac{1}{2}) = \{1 + (\alpha^2/n^2)/(1-\alpha^2/n)\}^{-\frac{1}{2}} = \{1 + (\alpha^2/n^2)(1+\alpha^2/n)\}^{-\frac{1}{2}} \quad (13)$$

Expanding these like in (8) generates a parabola for H of the required Kratzer form (6), since

$$\begin{aligned} E_{n, \frac{1}{2}} / \mu c^2 &= [f(n, j) - 1] = \{1 + (\alpha^2/n^2)(1+\alpha^2/n)\}^{-\frac{1}{2}} - 1 \\ &= -\frac{1}{2}(\alpha^2/n^2)(1+\alpha^2/n) + \frac{3}{8}(\alpha^4/n^4)(1+\alpha^2/n)^2 - \dots \approx -\frac{1}{2}\alpha^2/n^2 - \frac{1}{2}\alpha^4/n^3 + \frac{3}{8}\alpha^4/n^4 - \dots \\ &= (-\frac{1}{2}\alpha^2/n^2)[1 + \alpha^2(1/n - \frac{3}{4}/n^2) - \dots] \end{aligned} \quad (14)$$

In first order, the final parabolic compact energy level equation for H becomes

$$\begin{aligned} E_{n, \frac{1}{2}} &= (-\frac{1}{2}\mu\alpha^2 c^2/n^2)[1 + \alpha^2(1/n - \frac{3}{4}/n^2) - \dots] \\ &= (-R/n^2)[1 + \alpha^2(1/n - \frac{3}{4}/n^2) - \dots] \end{aligned} \quad (15)$$

much more accurate than Bohr's leading 2D $-R/n^2$ term, still preserved. It is too easily forgotten that bound state formula (15) is due to Sommerfeld, not to Dirac, and that it remains at the basis of modern bound state QED [24].

With (15) and numerical dimension-less ratio $-E_{n, \frac{1}{2}}/R$, errors δ_n for Bohr theory like Δ_n in (5) are easily quantified by a clearly visible quartic (in cm^{-1})

$$\delta_n = -E_{n, \frac{1}{2}} - \frac{1}{2}\mu\alpha^2 c^2/n^2 = \alpha^2 R(1/n - \frac{3}{4}/n^2)/n^2 \text{ cm}^{-1} \quad (16)$$

for H $np_{\frac{1}{2}}$ states. This justifies equations (4c) and (5a-b), the curves in Fig. 2 and in [1,3] but also gives the attractive term $-\alpha^2 R/n^3 = -5,84/n^3 \text{ cm}^{-1}$ needed to remove the STR errors in Fig. 2d (see above).

Sommerfeld-QED quartic (16) transforms in numerical variants $\delta_n/R\alpha^2$, $n\delta_n/R\alpha^2$ and $n^2\delta_n/R\alpha^2$, shown in Fig. 3. The Mexican hat shape shows only with extrapolation as in Fig. 2. Using (16), cubic $n\delta_n/R\alpha^2$ is harmonic between a parabola with n^0 and a quartic with n^2 , since $n\delta_n/R\alpha^2 = \sqrt{[(\delta_n/R\alpha^2)(n^2\delta_n/R\alpha^2)]}$ and explains why all curves converge to the same critical points (Fig. 3). With Sommerfeld's, unjustly called Dirac's equations (14)-(15), running Rydbergs (4c) are parabolic

¹⁵ Einstein's original non-sinusoidal orthogonal STR (1d) can be modified for bound H states with an amended form like $f(\alpha/n) = [1 + (\alpha/n)^2/\sqrt{(1-\alpha^2/n^2)}]^{-\frac{1}{2}} = [1 + \alpha^2(1+\alpha^2/n)/n^2]^{-\frac{1}{2}}$, the parabolic Sommerfeld variant hidden in (14)-(15). This variant suggests that the real harmonic H field would derive from a series expansion of a series.

$$R(n) \approx R[1 + \alpha^2(1/n^{-3/4}/n^2)] \quad (17)$$

as argued in [2]. With $R=109677,5854 \text{ cm}^{-1}$ as in (5e) and (7) for $np_{1/2}$, Rydbergs and energies become

$$R(n) \approx 109677,5854 + 5,8405/n - 4,3805/n^2 \text{ cm}^{-1} \quad (18a)$$

$$-E_{n,1/2} = -4,3805/n^4 + 5,8405/n^3 + 109677,5854/n^2 \text{ cm}^{-1} \quad (18b)$$

in perfect agreement with fit (5e). Before 1947, this impressive precision for H got Sommerfeld's, not Dirac's, bound state theory (15) even the status of an absolute theory. This had major consequences for metrology, based on the Rydberg $m_e \alpha^2 c^2$, still in vigor today [23]. It is evident that Sommerfeld¹⁶ is responsible for this status, since he succeeded in safeguarding Einstein's highly praised STR formalism for bound states. Unfortunately, the obvious link with H boson behavior and its possible impact for H polarization was never made. The irony is that Sommerfeld almost unwillingly proved that simple oscillating H fields (1a-c), say a simple cosine law, are far better than Einstein's original orthogonal STR field, which, by definition, can never cope with polarization (see above).

Hidden Kratzer oscillatory potential and harmonic Rydbergs in fermion-boson system H

With this pragmatic origin of the famous double square root equation (10), Kratzer's potential (6), showing in (10)-(11), retains its classical (boson) implications even when superimposed on fermionic H (see Appendix). Apart from factor α^2 and a shift, Sommerfeld-Kratzer potentials (6) and (15) give

$$-(1-n_0/n)^2 = -1 + 2n_0/n - n_0^2/n^2 \sim +1/n^{-3/4}n^2 \quad (19)$$

The numerical Kratzer parabola (6) hidden in H $np_{1/2}$ refers to a critical n-value $n_0=3/2$, half integer and constant, instead of running $\ell=n-1$. The Kratzer potential needed for $np_{1/2}$ -states becomes

$$E_p = -(1/3)(1-n_0/n)^2 = -(1/\sqrt{3} \cdot 1/2 \sqrt{3}/n)^2 = -1/3 + 1/n^{-3/4}n^2 \quad (20)$$

which, in turn, refers to a different asymptote E'_p , shifted numerically by

$$E'_p = -(1/3)(1-n_0/n)^2 + 1/3 = -1/3(1-1) + 1/n^{-3/4}n^2 = +1/n^{-3/4}n^2 \quad (21a)$$

This asymptote shift can be dealt with using classical physics and remains mathematically exact using a virtual particle-antiparticle pair asymptote difference $(1-1)/3$ in (21). This freedom of asymptote for H is connected with the form of Kratzer's oscillatory potential (6), i.e. with or without constant asymptote shift, governed by n_0 in (6).

An important aspect of asymptote shifts, never mentioned in bound state QED and by NIST [2], is the appearance of harmonic Rydbergs R_{harm} . For H $ns_{1/2}$, $R_{\text{harm}}=109679,3522 \text{ cm}^{-1}$, while for $n=1$, the ground state, $R_1=109678,7737 \text{ cm}^{-1}$ [2] (see also below). For $np_{1/2}$ with (21), shift $\alpha^2 R/3 = 1,94 \text{ cm}^{-1}$ gives $R'_{\text{harm}} 109677,58 + 1,94 = 109679,52 \text{ cm}^{-1}$, whereas for its ground state at $n=1$, shift $\alpha^2 R/4$ gives $109679,04 \text{ cm}^{-1}$. The R-parabola in Fig. 2a learns that underlying linear H field of type $a-b/n$ or $\sin(1/2\theta)\sqrt{2}$ (see around Fig. 2), never discussed in bound state QED, will have to be understood from

¹⁶ It is too easily forgotten also that Sommerfeld's work was much admired. For 1901-1950, this got him the highest number of nominations (81) for a Nobel prize but never received it (Bohr got 20 nominations) [25]. A. Kratzer and E. Fues but also P. Debye, W. Pauli, W. Heisenberg and H. Bethe belonged to Sommerfeld's *school* (<http://www.lrz-muenchen.de/~sommerfeld>).

first principles in ab initio H polarization theory [26]. For np, R'_{harm} is shifted by $\alpha^2/3$, which is important to understand observed distorted quartics, extracted from the lines. Fig. 4 shows that the invisible theoretical harmonic quartic δ_n , scaled with α^2 , or

$$\delta_n/(\alpha^2) = (1/3)(1 - 1.5/n)^2/n^2 \quad (21b)$$

is symmetrical and critical at $n=3$, whereas the clearly visible observed anharmonic quartic

$$(1/3)[(1 - 1.5/n)^2 - 1]/n^2 \quad (\text{giving observed } +1/n^3 - 3/4/n^4 \text{ after inversion}) \quad (21c)$$

is not only asymmetrical but also its shape is markedly different. This also shows how linear asymptote shifts can affect the shape of the quartics, hidden in the H line spectrum, as argued above.

Exposing harmony with parabolas relies on scaling effects on coefficients and the value of asymptotes. Forms $(a-b/n)^2 = a^2[1 - (b/a)/n]^2 = b^2[(a/b) - 1/n]^2 = 2ab[\sqrt{(1/2a/b)} - \sqrt{(1/2b/a)}/n]^2$ are all equivalent. Rewriting the latter with ratio $r = (b/a)$ gives harmonic relation $2(ar)^2(1/2/r^2 - 1/n + 1/2r^2/n^2)$ as it is observed (21c).

However, exposing details on H symmetries also suffers from the natural limits imposed on observation. Due to (1e), observable lines are limited to the quantum domain between $n=2$ and $n=\infty$ (or between $1/n=0.5$ and $1/n=0$) as indicated with the 2 vertical lines in Fig. 4.

With this natural limitation of (1e), it is apparent that, to expose all the details of harmonic H-behavior (boson symmetry), extrapolation¹⁷ beyond this observable region is essential [3], as argued also above. These details all derive from Sommerfeld's decision to introduce Kratzer's oscillator potential (6) in a bound state H theory. This important Sommerfeld-Kratzer connection on classical rotator-oscillator (now fermion-boson) physics is never mentioned in the history of H bound state QED. On the contrary, QED, the QFT for the electromagnetic field, is connected almost exclusively with Dirac¹⁸. Sommerfeld's double square root equation (10) cannot but refer to Mexican hat curves for bound Coulomb H states, whereas the link between quartics and chirality was known already with 19th century chemistry [27-28].

Why all this was nevertheless persistently overlooked in QED, is difficult to understand: it was well known that radiation cannot but act like a boson system, which exhibits chiral behavior. This makes oscillator contributions (6) for resonant polarized H-states quite plausible, the more since also polarization angles or phases were already available with de Broglie's (1f).

At this stage, it is not yet evident to correlate quartic (16) with chiral behavior of polarized H, since quartics apply for most transitions in 2 level systems like order-disorder transitions (see below).

A direct link between H spectrum and H polarization like in Fig. 1a, can only be provided if and only if critical de Broglie polarization angles 90° and 180° are retrieved exactly from the H line spectrum.

¹⁷ Bohr theory is based on extrapolation too to get at ground state $n=1$ in a wavenumber or $1/\lambda$ view. This avoids the infinity with (1e) for state $n=1$ in a wavelength or λ view (Angstrom), the spectral unit in vigor in the 19th century.

¹⁸ In the latest review on H bound state QED [24], Dirac is mentioned 116 times, Sommerfeld and Kratzer not once.

H polarization and H chirality: PDW shifts and spectral signatures for \underline{H}

Quantitative signatures for H polarization, and hence for natural \underline{H} , only appear with the Lyman $ns_{1/2}$ series. With $j+1/2=1$, these states also comply with Sommerfeld's secondary quantum condition $\ell=n-1$. If (15) were the result of an absolute theory, as commonly believed at the time, $ns_{1/2}$ should be degenerate with $np_{1/2}$ and both should obey (18).

This theoretically predicted degeneracy was, however, flawed for interval $2S_{1/2}-2P_{1/2}$ by Lamb and Retherford [29]: the terms differ by more than 1000 MHz or $0,035 \text{ cm}^{-1}$, in line with what many other physicists already suspected earlier [29]. Immediately after its publication in 1947, the shift caused a great turmoil in theoretical physics, since the almost sacred, so-called absolute Sommerfeld-Dirac formula (10) and (15) proved wrong. The shift initiated the search for a new physics and later, following Bethe's first explanation for the shift [30], led to modern quantum field theories and eventually the Standard Model as we know it today. How important the Lamb shift may have been for theoretical physics [16,24], it is even more important for the fate of natural \underline{H} , although this was never mentioned, until 2002 [2]. Its importance becomes apparent with $ns_{1/2}$ fit (5d)

$$-E_{ns_{1/2}} = -4,3651/n^4 + 5,5522/n^3 + 109677,5868/n^2 \text{ cm}^{-1} \quad (22)$$

with slightly different higher order coefficients than in (18) [2]. These small differences correspond with the Lamb-shifts between the 2 series.

Instead of critical $n_0=3/2$ for $np_{1/2}$, the derivative of (22) leads to a critical n_0 for its Kratzer potential (6) and for its running Rydbergs $n^2 E_{ns_{1/2}}$ at [2]

$$n_0 = 1,572 \approx 1/2\pi \quad (23)$$

Reminding polarization Fig. 1a, phase (23), typical for orthogonal models with complementary sine and cosine of the same angle like Bohr's, is nevertheless also the critical angle for circular H polarization, pointing towards left- and right-handed configurations H and \underline{H} .

The Sommerfeld-Kratzer super-symmetric quartic correction for H Lyman $ns_{1/2}$ gives for shifts (2c)

$$\text{HPDW shifts} \sim (1/\sqrt{\pi-1/2}\sqrt{\pi}/n)^2/n^2 = (1/\pi)(1-1/2\pi/n)^2/n^2 \quad (24)$$

instead of quartic (16) and parabola in (20) for $np_{1/2}$. Classically, and apart from trivial $n_0=\infty$, this quartic for H PDW shifts is not only critical for $n_0=1/2\pi$ in (23) but also for $n_0^2=\pi$, instead of $3/2$ and 3 for $np_{1/2}$. This shift in critical behavior for $ns_{1/2}$ provides with the 2 ultimate spectral signatures for H polarization and for natural \underline{H} . With quartic (24), not only $1/2\pi$ in (23) for circular H polarization but also critical angle of π or 180° for linear H polarization shows up unambiguously as

$$n_0^2 = \pi \quad (25)$$

as with de Broglie's theoretical polarization angles (1f).

This finally proves that observed H wavelength shifts, i.e. errors with respect to Bohr 2D fermion $1/n^2$ theory, are polarization dependent wavelength (PDW) shifts in important H Lyman's $ns_{1/2}$ -series. Angle (25) for a simple Coulomb H bond provides with an absolute, generic signature for an internal permutation (by rotation), i.e. an inversion on the axis from \rightarrow , say $+1$, to \leftarrow , say -1 . Without (strong)

external fields or with data extrapolated to zero-field (Lamb-Retherford) and with oscillations projected on a Coulomb field axis, inversion (25), implicit with (1a), i.e. H acting as a half wavelength plate in de Broglie theory (1f), must take place between the 2 charges, conventionally assigned to electron and proton, which formally become anti-electron (positron) and antiproton. If state +1 stands for a natural, stable Coulomb H-state with attraction $-e_1e_2/r$, inverse -1 must stand for a natural stable Coulomb \underline{H} -state with attraction $-e_2e_1/\underline{r}$.

Nevertheless, natural \underline{H} is still forbidden by the physics establishment, while bound state QED uses the very same Sommerfeld quartic generating field equation (10). Failing to see critical H phase¹⁹ $1/2\pi$ and π , hidden in de Broglie's equation, at an earlier instance had devastating consequences for physics [1]. Apart from an unjust ban on natural \underline{H} , many other important issues are affected: CPT, WEP, existence of antimatter, cosmology, hole-theory, Dirac sea, matter-antimatter asymmetry, Big Bang, $\underline{H}\underline{H}$ bonding, $\underline{H}\underline{H}$ oscillations, geometric phase, phase transitions, entanglement.... [1,21].

Results

(i) Precision

To test the reliability of and the precision behind the π -dependence for the $ns_{1/2}$ series, compared with that on 3 for the $np_{1/2}$ -series, we verify that, with (20) and (24), parabolic Rydberg ΔR corrections are

$$\Delta R(np) = \alpha^2 R (1/\sqrt{3} - 1/2 \sqrt{3}/n)^2 = +1,946827 - 5,840480/n + 4,380360/n^2 \text{ cm}^{-1} \quad (26a)$$

$$\Delta R(ns) = \alpha^2 R (3/\pi) (1/\sqrt{\pi} - 1/2 \sqrt{\pi}/n)^2 = +1,775293 - 5,577248/n + 4,380360/n^2 \text{ cm}^{-1} \quad (26b)$$

with $\alpha^2 R = 109677,58545/137,035999^2 = 5,840480 \text{ cm}^{-1}$. In as far as a number 3-based n-theory (26a) is of first principles character, a rescaled version with π instead of 3 is a derived first principle's theory also, as evident with (26b). The theoretical Rydbergs are plotted versus the observed ones Fig. 5.

Linear fits give

$$R(np) = 109679,533968 - 1,001024 \Delta R(np) \approx 109679,533968 - \Delta R(np) \quad (27a)$$

$$R(ns) = 109679,353174 - 0,995566 \Delta R(ns) \approx 109679,353174 - \Delta R(ns) \quad (27b)$$

The 2 harmonic Rydbergs differ by $109679,53 - 109679,35 = 0,18$. With (26ab), level energies become

$$-E(np) = (109679,533968 - \Delta R(np))/n^2 = 109677,5854/n^2 + 5,840480/n^3 - 4,380360/n^4 \text{ cm}^{-1} \quad (28a)$$

$$-E(ns) = (109679,353174 - \Delta R(ns))/n^2 = 109677,5854/n^2 + 5,577248/n^3 - 4,380360/n^4 \text{ cm}^{-1} \quad (28a)$$

which give an absolute error of 2,04 and 0,64 MHz for ns and np respectively. Using the fits in (27), the errors reduce to 0,24 and 0,18 MHz (some $0,000007 \text{ cm}^{-1}$) as shown in Table 2. Part of the remaining small errors is due to adaptations in constants and conversion factors since [15].

To the best of my knowledge, this is by far the simplest accurate *one-parameter* theory ever to account for observed Lamb-shifts from first principles. The explanation for the Lamb shift in standard QED is one of the most complex exercises in theoretical physics. This complexity shows when it comes to

¹⁹ Herbst [31] uses critical $1/2\pi$ as a Friedrichs extension for a one-particle Hamiltonian in Coulomb potential $V(x) = -n_0/n$, with lower bounds $E \geq mc^2 \sqrt{1 - (1/2\pi n_0)^2}$ in the range $0 \leq n_0 < 2/\pi$ (see [32] for a discussion).

calculate H line intensities, intimately connected with H polarization. Bound state QED is not a closed but an open theory, which adds to the ambiguity surrounding its labyrinth of terms created with the expansions for (10).

The rationale behind our simple solution for Lamb-shifts is H polarization, persistently but unjustly overlooked in QED/QFT [1].

(ii) The 21 cm H line and natural \underline{H}

The two harmonic quartics for the Lyman $ns_{1/2}$ - and $np_{1/2}$ -series are shown in Fig. 6 but an important observed internal anchor for H is added, the 21 cm line. The observed hyperfine splitting of ground state $1S_{1/2}$ 1420,4058 MHz (21,1061133 cm) is 0,04737964 cm^{-1} , as in Fig. 6 (horizontal line). This usually faint line, important for cosmology, is easily measured, since H is so dominant in the Universe (CBR). It is easily computed in QED with electron and proton magnetic moments. However, QED cannot place this line, important for H-related polarization effects in the Universe, within the context of a polarized H atom, where it really belongs, since QED is internally inconsistent exactly where it matters: H polarization.

Barrier-heights in its Mexican hat curves reflect all of the basic symmetries in H. Fig. 6 shows that the famous 21 cm line is exactly in between barriers in $ns_{1/2}$ - and $np_{1/2}$ -quartics, with respective heights 0,044649 at $n=\pi$ and 0,054273 cm^{-1} at $n=3$. This novel but unexpected result again calls for a generic H polarization or CSB theory, with due respect for this 21 cm line [26].

(iii) Role of π in quantum rules and de Broglie quantization

Kratzer's potential allows rotations and/or oscillations (see Appendix), while Bohr's theory only gives rotations. Their difference must show in quantum rules. In Bohr's quantum hypothesis

$$(mvr)_B = n\hbar \tag{29a}$$

Planck's quantum of action \hbar is scaled with the circumference of a unit circle 2π , giving h . Since quantum numbers are projections on the axis, Bohr's hypothesis hides the possibility that, for linear H, oscillations along an axis obey a rescaled quantum hypothesis of type

$$(mvr)_{SK} = (k/2\pi)h \tag{29b}$$

which could be called the Sommerfeld-Kratzer quantum hypothesis, if it were not already available with de Broglie's quantum recipe for fields (1e). Obviously, k is related to Bohr's n by scaling only or

$$k = n/2\pi \tag{29c}$$

in line with de Broglie's (1e) and appears with Rydbergs R_{SK} or H-state energies scaled accordingly.

Results (29a) and (29b) warn against improper use of \hbar in so-called absolute theories with $\hbar=c=1$.

For a de Broglie state with $n=\pi$, i.e. for the classical anchor of H in the ns -series, $k=1/2$ is a constant half integer quantum number, not only typical for H harmony but also for H, acting as a half wavelength plate. In second order, this value is also given away by half integer spin for fermions and is exposed as such by atom H, when its spectrum is measured in (strong) external fields.

If H harmony were expressed with $n=\pi$ or $k=1/2$, harmonic scale factor $1/\pi^2$ affects conventional H views by a factor of some $1/10$. Conventional recoil being 60 cm^{-1} ($109677,58/1836 \text{ cm}^{-1}$), recoil in a de Broglie harmonic state is only 6 cm^{-1} , close to $\alpha^2 R=5,84 \text{ cm}^{-1}$ in (26a). We return to all this in [26].

(iv) Classical phase transition in atom H

Inversion within system H at critical $n=\pi$ implies that a phase transition occurs from state $+1$ or phase $\theta=0$ to state -1 or phase $\theta=\pi$, the rationale behind the H quartics or Mexican hat curves above.

If not bound to chirality, double well curves give away an internal phase transition in a 2 level quantum system (order-disorder, state of aggregation...). These H potential energy curves (PECs) are obtained with energy differences, i.e. H PDW shifts, plotted versus $1/n$ (see Fig. 1 in [3]). Taking energy differences from the Bohr ground state $n=1$ gives the slightly distorted Mexican hat curve of Fig. 7a, instead of the harmonic quartic for H PDW shifts with the harmonic Rydberg [3]. To illustrate the effect of asymptote of R-shifts, curves for intermediate and more extreme $R>R_{\text{ham}}$ are also shown. However, when these same small energy differences, i.e. H PDW shifts, are plotted versus n as in Fig. 7b, the resulting curves not only lose their typical harmonic quartic shape. Quite surprisingly, typical Vander Waals-Maxwell patterns show up for all curves in the H quantum interval $n=1$ to $n=\infty$. The upper continuous curve for ideal behavior, i.e. the ideal gas law of the 19th century, refers to the ideal Coulomb law in Bohr's version $-R/n^2$ for the quantum world. The relevance of Fig. 7b is improved with the 21 cm H line included as reference. The inverted Van der Waals n -view in Fig. 7b calls for an explanation of the H system with density fluctuations upon compressing the original electron-proton system by decreasing their separation [5, 33].

Mass or density fluctuations along the radial Coulomb field axis are usually not considered but readily appear when with reduced mass, instead of total mass (see Appendix). Moreover, the procedure applied to go from the H quartic in Fig. 7a to the Vander Waals-type curve in Fig. 7b is readily inverted. To get at a classical Vander Waals curve in a P,V diagram, pressure data P are plotted versus volume V, as in Fig. 7b. The classical Maxwell, double well or Mexican hat curve immediately shows when plotting the same pressure data versus $1/V$ instead, as in Fig. 7a [33].

Since critical points in the H spectrum in whatever analytical relation refer to relative contributions of fermion and boson symmetries in H, the puzzling result in Fig. 7b must relate to atomic BECs (Bose-Einstein condensates) [33]. With this phenomenological analysis, a striking one-by-one correlation appears between (i) macroscopic 19th century Vander Waals-Maxwell behavior of neutral systems with 2 phases (water-ice for H_2O) and their classical phase transition and (ii) the microscopic phase transition between two different phases H and $\underline{\text{H}}$ of the same two level quantum system, natural and neutral atomic species hydrogen [33].

Discussion

H-signatures (23) and (25), theoretically allowed by de Broglie's standing wave equation, were already overlooked in the earliest days of quantum field theory and especially in the aftermath of the Lamb-shift. If the H line spectrum were interpreted along these lines, a theoretical ban on natural H and on HH would never have appeared. In QFT, handedness or helicity is connected with particle spin $\pm 1/2$ in a dynamic approach. Yet, with quantum condition $j+1/2=1$ for equation (10), dynamic effects of half integer spin vanish, which means that parabolic, sinusoidal variations (23) for the $ns_{1/2}$ series of natural, neutral and stable species H can only be accounted for with a generic H polarization or CSB theory, classically and quantitatively in line with cosine law (1) for 2 internal harmonic H fields. This model underlies our Bohr-like H polarization theory (2a) in beta-version [26]. To the best of my knowledge, no ab initio H polarization theory exists today (see Introduction). In a first principles theory, field ratio a/b and fractional polarization angle θ in (1a-c) must be identified analytically [26].

The use of more or less constrained Bohr and Kratzer potentials reduces to physical differences between mathematically equivalent descriptions of circles (see Appendix). In Bohr's standard central field approximation, a circle is described with a freely rotating radius r (0,+1) and a phase of 90° between 2 orthogonal fields (radial and angular fields or static and dynamic fields). In the mathematically equivalent bipolar view, the circle is described with a diameter $2r$ and two poles (+1,-1) with a phase of 180° between 2 parallel or antiparallel fields (linear 2 field case, electron- and proton Coulomb fields), as suggested with de Broglie's equation (1g). In [26], we analyze 2 internal sub-field models: (i) cosine law (1a), which implies sinusoidal fluctuations between field sum and field difference, both having different directions in space and (ii) its linear bipolar variant $a\cos\alpha+b\cos\beta$, for which $a\sin\alpha=b\sin\beta$ and $(\alpha+\beta)=\pi-\theta$, which implies fluctuations of the origin instead (vacuum fluctuations). These equations appear for all harmonic periodic motions, governed by $\cos\alpha+\sin\beta$. Equivalent numerical field equations (1a-c) for H, add to the confusion about the improper use of reduced mass in bound state QED (10), as remarked above, in the Appendix and referred to in [34]. In fact, for harmonic reduced mass to appear in bound state theories on a gravitational basis, total mass m_H looses its scalar behavior (see Appendix). The rationale is that recoil transforms exactly from multiplicative to additive in

$$1/(1+m_e/m_p) \equiv 1 - m_e/m_H \quad (30a)$$

which is important for field sum and difference in (1c) [26]. The derived symmetry behind (30a) for reduced mass leads to

$$(1+m_e/m_H)/(1 - m_e/m_H) = 1,0011\dots \quad (30b)$$

numerically close the anomalous electron mass [2]. In this form, H line splitting in function of

$$1 \pm m_e/m_H \quad (31)$$

would make total H mass m_H indirectly responsible for the breaking of left-right symmetry for boson system H and, by extension, for a 2 unit charge Coulomb bond between 2 fermions. Not surprisingly,

this is consistent with observation as argued before on a phenomenological basis [34]. An objection to (31) could be that recoil $(m_e/m_p)R$ gives about 60 cm^{-1} , too large to account for the H observed oscillations in QED of order $\alpha^2 R \approx 6 \text{ cm}^{-1}$ or 10 times less. This conventional argument on recoil is, however, deceptive for harmonic H states, as shown in the foregoing paragraph.

An argument in favor of recoil²⁰ as a symmetry breaker is that its oscillations with frequency ω , instead of rotations with angular frequency $\omega/2\pi$, compares well with a rescaled fine structure constant, although this effect is not manifest in de Broglie's original standing wave equation (1e).

Confronting Coulomb and radiative fields e^2/r and $h\nu=hc/\lambda=2\pi\hbar c/\lambda=2\pi(e^2/\alpha)/\lambda$ gives

$$\lambda/r=2\pi(e^2/\alpha)/e^2=2\pi/\alpha= 6,28\cdot 137= 861 \quad (32)$$

the hidden scale factor behind de Broglie's variant (1f). We notice that twice recoil is $(1836/2)=918$ gives a difference of about 57 with (32) but also that $\alpha/2\pi=r/\lambda$ in (32) appears as the leading term in the Schwinger expansion for the so-called anomalous electron mass [35]. Corrections for anomalous electron mass are also used in bound state QED [24], which strengthens the confusion about the real role, played by recoil. With (32), a bound Coulomb state, obeying virial $\frac{1}{2}e^2/r_0$, will absorb a frequency λ_0 , deriving from

$$\frac{1}{2}\lambda_0/r_0=4\pi/\alpha=2\cdot 861=1722 \approx 1836 \quad (33)$$

a field scale factor, perfectly compatible with inverse recoil $1836/1$.

These strange but unavoidable consequences for recoil, fine structure constant and number π must all be seen in a context of H polarization and of the de Broglie standing wave equation (1e). Combining these intriguing elements and using first principles will result in a generic, system independent polarization theory, easily applied to H and compatible with the equations above [26].

Conclusion

For more than 50 years and without any difficulty, theorists admitted that the H Lyman $np_{1/2}$ -series is based on numbers (ratios, proportions, symmetries) 1,5 and 3 deriving from Sommerfeld-Dirac QED equation (10). If so, theorists should have no difficulty either to admit that a slightly different H Lyman $ns_{1/2}$ -series relies on slightly different numbers $\frac{1}{2}\pi$ (1,57) and π (3,14), given already away with de Broglie's equation, when interpreted in terms of polarization angles (phases). These small differences account for the observed Lamb-shifts and were, eventually, responsible for major new developments in theoretical physics, where polarization remains a central issue. There is a world of difference between the two sets of critical data for the same stable system H: only with de Broglie or Lamb-numbers $\frac{1}{2}\pi$ and π , natural phenomenon polarization appears for the H Coulomb bond but, for reasons extremely difficult to understand, this was never appreciated in the past [1-5].

²⁰ Instead of R in cm^{-1} , recoil for $1/R$ in cm or Å, equal to $10^8/109677,58=911,7633 \text{ Å}$, gives $911,7633/1836,15267 = 0,49656 \text{ Å}$ of the expected numerical magnitude, reminding $r_H=r_e+r_p=r_e(1+m_e/m_p) \text{ Å}$, with $R=1/2e^2/r_e \text{ cm}^{-1}$ but $1/R=2r_e/e^2 \text{ cm}$. We return to this problem elsewhere [26].

On the experimental side, H polarization theory must have access to as much as possible precisely measured H Lyman terms, more than the few available today like [36]. Since line profiles are not only affected by PDW shifts, line intensities should be measured also with great precision, since it proves extremely difficult to calculate intensities with present bound state QED. If there is any logic in the analysis above, H polarization must affect H line intensities, which should also exhibit critical behavior (fluctuations) at the critical n-values, given above. In the end, a family of related H lines with the same rotational symmetry is more useful to disclose H chiral behavior than a single line²¹. This puts question marks on the artificial \underline{H} -experiments at CERN to get at single line 1S-2S, as argued before [5]. Rather than pursuing their impossible dream with artificial \underline{H} , the physics community would be better served with many more H lines and their profiles, measured with the greatest precision possible. The history of quantum theory before Schrödinger's time (Bohr-Sommerfeld-Kratzer-Compton-de Broglie) and of bound state QED, the observation of the Lamb shifts, the CBR line,... easily falsify the unjust fate of natural \underline{H} . Although QFT prescribes H Mexican hat curves and uses these typical bound state patterns at length in the SM to understand elementary particle behavior and chirality, it has persistently failed to make this obvious connection for the most essential [16] element hydrogen: H quartics, H polarization and H chirality must all be intimately and quantitatively connected. It is undeniable that errors of 2D Bohr $1/n^2$ fermion theory classify as sinusoidal polarization dependent wavelength (PDW) shifts, in line with Compton's non-resonant X-ray experiments and de Broglie's equation. Unambiguous spectral signatures for natural \underline{H} , $1/2\pi$ and π , only show for the Lamb-shifted H Lyman $n_{s/2}$ series. While QED uses the very same quartic-generating double square root Sommerfeld-Kratzer function for atom hydrogen, it nevertheless puts a ban on natural \underline{H} , which classifies QFT as internally inconsistent on neutral antimatter²².

Acknowledgements

I am in debt for correspondence to R.L. Hall (Kratzer potential), to R. Casini and R.M. Sainz (H line profiles) and to G. Vanden Berghe for discussions on Ramanujan's work.

Appendix. Kratzer potential and reduced mass fluctuations in fermion-boson system H

Chemists know for long that, in composite quantum systems, rotations interfere with vibrations and hope to find a universal potential to explain the order observed for molecular spectroscopic constants [19,20]. In this respect, simple molecular Kratzer potential (6) is superior to Morse's [19]. Numerically equivalent forms are

$$V(n) = -A/n + B/n^2 = A(-1/n + (B/A)/n^2) = (-A/n)(1-b/n) \quad (A1)$$

Eqn. (A1) appears for running Rydbergs (17) in Sommerfeld H theory (see text). With $A=-e^2$; $n=r$ and $A=hc$; $n=\lambda$, (A1) can apply for Coulomb and radiative fields, either for unit mass systems ($m=1$) or for systems without specifying particle masses. In this more general view, Coulomb field $-e^2/r$ becomes

$$V(r) = -e^2/r + b/r^2 \quad (A2)$$

Particle mass does not show but must behave in an harmonic way, the problem for this Appendix.

²¹ Trying to determine handedness for a single line requires that absolute handedness is assessable, which is still impossible.

²² If so, my claim for the discovery of natural \underline{H} [4] should be validated.

Putting the first derivative of (A1) equal to 0 at critical separation r_0 gives $e^2/r_0^2 - 2b'/r_0^3 = 0$, which means

$$b = \frac{1}{2}e^2r_0 \text{ and } V(r_0) = -\frac{1}{2}e^2/r_0 \quad (\text{A3})$$

Shifting the asymptote to make the minimum coincide with 0, natural difference potentials for Coulomb $-1/r$ and radiative $+1/\lambda$ fields become

$$\begin{aligned} V(r) - V(r_0) &= -e^2/r + \frac{1}{2}e^2r_0/r^2 + \frac{1}{2}e^2/r_0 = (\frac{1}{2}e^2/r_0)(1 - r_0/r)^2 = A(1 - n_0/n)^2 \\ V(\lambda_0) - V(\lambda) &= hc/\lambda - \frac{1}{2}hc\lambda_0/\lambda^2 - \frac{1}{2}hc/\lambda_0 = (-\frac{1}{2}hc/\lambda_0)(1 - \lambda_0/\lambda)^2 = -A'(1 - n_0/n)^2 \\ -[V(\lambda_0) - V(\lambda)] &= A'(1 - n_0/n)^2 \end{aligned} \quad (\text{A4})$$

the basis behind (6) and which leads to the different parabolic equations, discussed in the text.

Unconstrained by mass, second order Kratzer term $|b/n^2|$ represents in a generic way the harmonic relations between frequency and wavelength $\nu\lambda=c$ for radiation, between frequency and separation $\omega r=v$ for oscillations in linear and between angular frequency ω and radius r for rotations in circular systems

$$d(-e^2/r)/dr = +e^2/r^2; \quad d\nu/d\lambda = -c/\lambda^2; \quad d\omega/dr = -v/r^2 \quad (\text{A5})$$

These harmony relations (A5) justify Kratzer's second order term $\pm b/n^2$.

The 2nd derivative for $r=r_0$ gives force constants k for harmonic systems, still without specifying masses. In fact, $d^2V(r)/dr^2 = -2e^2/r^3 + 6b/r^4 = -2e^2/r^3 + 3e^2r_0/r^4$ returns k equal to

$$k_C = +e^2/r_0^3 \text{ and } k_R = +hc/\lambda_0^3 \quad (\text{A6})$$

for attractive harmonic Coulomb and radiative fields, consistent with (A4). With (A6), Kratzer's procedure obeys Hooke's law $-\frac{1}{2}kr^2$ for harmonic equilibrium, since $-\frac{1}{2}kr_0^2 = -\frac{1}{2}e^2/r_0$ as it should.

This brings us to Kratzer's treatment of harmonic particle mass. For bound, stable systems with masses in harmonic motion and with periodicities governed by sine and cosine, force constant k for inverse harmonic fields relates to reduced mass μ with frequency ω

$$k = \mu\omega^2 \text{ or } \omega = \sqrt{k/\mu} \quad (\text{A7})$$

Reduced mass $\mu = m_1m_2/(m_1+m_2) = m_1m_2/M$ applies for any complementary mass system $M = m_1+m_2$. The only constraint on particle mass in harmonic systems is that it requires reduced, not total mass. Theoretically possible generalized algebraic reduced mass fields are always of form²³

$$\mu = Mf(\gamma_{\pm}) \text{ or } \mu/M = f(\gamma_{\pm}) = \pm\gamma - \gamma^2 \quad (\text{A8})$$

Upon a real or virtual division of total mass m_H , reduced mass is no longer a scalar (see text). As with numerical polarization fields (1a)-(1c), the hidden numerical mass field

$$f(\gamma_{\pm}) = \pm\gamma - \gamma^2 \quad (\text{A9})$$

automatically imposes parabolic, if not sinusoidal behavior for any complementary mass (quantum) system. As a result, generic parabolic behavior of reduced mass or density fluctuations in (A9) resemble the curve in Fig. 2a for the running H Rydbergs. While $\gamma=0$ and $\gamma=1$ both stand for undivided total mass, but not for a system with zero total mass, $\gamma=1/2$ is the value for a perfectly symmetrically divided system with mass parts $1/2M$ each. With fermion-boson symmetries in mind, γ small ($\approx 1/1836$) but not equal to zero implies $1-\gamma \approx +1$ for its

²³ Reduced mass μ requires harmony for m_1 and m_2 : $\mu = m_1m_2/(m_1+m_2) = m_1m_2/M$ is equivalent with $\mu/M = m_1m_2/M^2$ or $\mu M = m_1m_2$. Scaling parts gives $\mu = (\gamma - \gamma^2)M = \gamma(1-\gamma)M$ since $m_1m_2/(m_1+m_2)^2 = m_1(M-m_1)/M^2 = (m_1/M)(1-m_1/M) = (\gamma - \gamma^2) = \gamma(1-\gamma)$ is exact. With the law of association, permutation $+1 = -m_1/M + (1+m_1/M)$ is valid but gives $-\gamma(1+\gamma)$ instead. This leads to algebraic reduced masses, as in reduced mass field $f(\gamma_{\pm})$ in (A8). An inverse view on mass $m_X = C/r_X$, used in classical and quantum physics, transforms linear mass relation $M = m_1+m_2$ into harmonic size $r_X = r_1r_2/(r_1+r_2) = r_1r_2/r_X$ or $r_X = \sqrt{r_1r_2}$, the basis of (1b) and (1c). The common sense behind complementary mass is that we can decide at will whether or not to divide a system: $M = m_1+m_2$ with $m_1=0$ (no bisection) returns M undivided but makes reduced mass zero (see [X] for a preliminary discussion). We deal with this important case of complementary systems elsewhere [26].

complementary part, which corresponds with fermion-behavior (Bohr-Kratzer view, rotations). Intermediary γ , near $\pm 1/2$, gives boson behavior (Kratzer view, oscillations). Looking at atom H as a boson gives reduced mass $\mu_H = 1/4 m_H$. While force constant k is usually considered a constant (like R in Bohr R/n^2 theory), this overlooks parabolic reduced mass effects, if not density fluctuations (A8). Harmonic mass-related effects, when real, will be reflected in observable frequencies of harmonic systems, by virtue of (A7).

To simplify the discussion and to avoid this extra degree of freedom of parabolic form for reduced, harmonic mass, associated with (A9), we proceed with Kratzer's potential in the hypothesis of constant reduced mass. With $v^2 = \omega^2 r^2$ and k_C in (A6), equilibrium for an harmonic Coulomb system with constant reduced mass obeys

$$\mu \omega^2 r_0^2 = \mu v^2 = e^2 / r_0 \quad (\text{A10})$$

Therefore, Kratzer's potential (6) not only gives equilibrium condition (A10) for mass-systems when in oscillatory harmonic motion but does not put constraints on the mass-distribution (reduced mass), which can apply for any value of γ in the domain $0 < \gamma < 1$. This includes extreme fermion as well as intermediary boson behavior for atomic system H.

In the former case, (A10) is formally degenerate with Bohr's first equilibrium condition for the rotating electron in the Coulomb field $\mu v^2 r_0 = e^2$ for radial velocity v on a Coulomb field axis. Bohr's central field approximation

$$V_{\text{Bohr}}(r) = -e^2/r + 1/2 \mu v^2 = -e^2/r + 1/2 \mu \omega^2 r^2 \quad (\text{A11})$$

led to valid rotator levels $E_n = (-1/2 e^2 / r_0) / n^2 = -R/n^2$, constrained by fermion behavior as well as by his quantum hypothesis (29a) for angular frequencies ω and angular velocities, perpendicular to the field axis. Bohr's potential (A11) does not relate to oscillations between complementary parts along a field axis, applying for boson-type harmonic H. The Kratzer potential is essentially an harmonic field for any harmonic system, divided in any harmonic way.

Kratzer boson-type oscillations in H rely on vibrations between 2 neutral, complementary parts of atom H, with maximum mass $1/2 m_H$ each. Bisecting H atom mass in the boson way is more classical, since it proceeds on a gravitational basis, difficult to understand at first sight but perfectly in line with classical equilibrium conditions $m_e r_e = m_p r_p$ or $m_e / m_p = r_p / r_e$ (see text). In a Coulomb view, bisection is achieved with 2 unit charges on 2 fermions, an extreme bisection of atom H in 2 complementary parts. A Bohr H-state $(-, +)$ with a charge conjugated fermion particle pair m_e, m_p (rotations) can nevertheless go over in an intermediate state with neutral boson particle pair $1/2 m_H, 1/2 m_H$ (oscillations), the classical rationale behind Sommerfeld's oscillatory corrections to the orthogonal STR field (see text) to end finally in a charge-inverted fermion state H $(+, -)$, the so-called forbidden state in QFT.

Whatever the meaning of (A9), harmonic Kratzer oscillations of boson type (6) on a single field axis can, nevertheless, interfere with Bohr rotations of fermion type with 2 orthogonal axes. When properly combined and scaled in composite fermion-boson system H, these lead to a Poincaré 3D polarization sphere for H and eventually, to the de Broglie polarization angles (1g), available for almost a century. We return to some of these problems elsewhere [26].

References

- [1] G. Van Hooydonk, Eur. J. Phys. D **35**, 299 (2005); physics/0506190
- [2] G. Van Hooydonk, Phys. Rev. A **65**, 044103 (2002); physics/0501144; Proc. PSAS2002, Ed.: S.G. Karshenboim, V.B. Smirnov, E.N. Borisov and V.A. Shelyuto, St Petersburg, 2002
- [3] G. Van Hooydonk, Acta Phys Hung. NS **19**, 385 (2004); physics/0501145; Proc. Wigner Centennial, Ed. M. Koniorczyk and P. Adam, Pecs, 2002
- [4] see for instance <http://www.physorg.com/news/3226.html>
- [5] G. Van Hooydonk, physics/0502074
- [6] A.H. Compton, Phys. Rev. **21**, 483 (1923)
- [7] L.A. Page, Rev. Mod. Phys. **31**, 759 (1959), M. Woods, Int. J. Mod. Phys. A **13**, 2517 (1998); hep-th/9802009; G. Moortgat-Pick et al., hep-ph/0507011
- [8] R.C. Jones, J. Opt. Soc. Am. **31**, 488 (1941)
- [9] H. Mueller, J. Opt. Soc. Am. **38**, 661 (1948)
- [10] N. Gisin and A. Go, Am. J. Phys. **69**, 3 (2001)
- [11] P. Zoller et al., Eur. J. Phys. D **36**, 203 (2005)
- [12] G.P. Agarwal, *Fiber-optic communication systems*, New York, Wiley, 2002; O.V. Belai et al. physics/0611039; V.I. Kopp et al., Science, **305**, 74 (2004)
- [13] N. Allard and J. Kielkopf, Rev. Mod. Phys. **54**, 1103 (1982), H. Margenau and W.W. Watson, Rev. Mod. Phys. **8**, 22 (1936)
- [14] R.L. Kelly, J. Phys. Chem. Ref. Data Suppl. **16**, 1 (1987)
- [15] G. W. Erickson, J. Phys. Chem. Ref. Data **6**, 831 (1977)
- [16] J.S. Rigden, *Hydrogen, The Essential Element*, Cambridge, Harvard University Press, 2003
- [17] A. Kratzer, Z. Phys. **3**, 289 (1920); Ann. Phys. **67**, 127 (1922)
- [18] A. Sommerfeld, *La constitution de l'atome et les raies spectrales*, 3d edition, Paris, Blanchard, 1923 (1st edition, *Atombau und Spektrallinien*, Braunschweig, Vieweg&Sohn, 1919)
- [19] G. Van Hooydonk, Eur. J. Inorg. Chem. **1999**, 1617 (1999)
- [20] G. Van Hooydonk, Spectrochim. Acta A **56**, 2273 (2000); physics/0001059; physics/0003005
- [21] G. Van Hooydonk, physics/0506190; physics/0508043; physics/0510108; physics/0511052; physics/0511115; physics/0512018
- [22] G. Boros and V.H. Moll, J. Comp. Appl. Math. **130**, 337 (2001); V.H. Moll, Not. Am. Math. Soc. **49**, 311 (2002). For S. Ramanujan, see <http://en.wikipedia.org/wiki/Ramanujan>
- [23] B. Cagnac, M.D. Plimmer, L. Julien and F. Biraben, Rep. Prog. Phys. **57**, 853 (1994)
- [24] M.I. Eides, H. Grotch and V.A. Shelyuto, Phys. Rep. **342**, 63 (2001); hep-ph/0002158
- [25] E. Crawford, *The Nobel Population: A Consensus of Nominators and Nominees for the Prizes in Physics and Chemistry 1901-1950*, Tokyo, Universal Academy Press, 2001, also at <http://physicsweb.org/articles/world>
- [26] G. Van Hooydonk, in preparation
- [27] G. Van Hooydonk, physics/0504040
- [28] F. Hund, Z. Phys. **43**, 805 (1927)
- [29] W. Lamb Jr. and W.C. Retherford, Phys. Rev. **72**, 241 (1947), Phys. Rev. **79**, 549 (1950)
- [30] H. Bethe, Phys. Rev. **72**, 339 (1947)
- [31] I. Herbst, Comm. Math. Phys. **53**, 285 (1977)
- [32] R.L. Hall and W. Lucha, J. Phys. A Math. Gen. **39**, 11531 (2006); math-ph/060259
- [33] G. Van Hooydonk, physics/0502098
- [34] G. Van Hooydonk, physics/0503133
- [35] J. Schwinger, Phys. Rev. **73**, 416 (1948)
- [36] M. Niering et al., Phys. Rev. Lett. **84**, 5496 (2000)

Table 1. Data for ns and np (terms [14] and energies [15]). Energies used for running Rydbergs $R_{II}(n)$ in (4c) and for quantum number differences for ns (5a) $10^6\Delta_n$ and (5b) $10^6\Delta'_n$ (all data in cm^{-1})

n	Terms ^{a)} ns	Terms np	$-E_{ns}$ ^{b)}	$-E_{np}$	$R_{II}(n)$ ns	$R_{II}(n)$ np	$10^6\Delta_n$ ns ^{c)}	$10^6\Delta'_n$ ns
1	(0)		(109678,773704)		109678,773704		0,0000	0,0000
2	82258,9559	82258,9206	27419,8178352	27419,8531233	109679,271341	109679,412493	1,1343	1,1343
3	97492,2235	97492,2130	12186,5502372	12186,5607410	109678,952135	109679,046669	0,2711	0,1808
4	102823,8549	102823,8505	6854,9188454	6854,9232846	109678,701526	109678,772554	-0,0823	-0,0411
5	105291,6329	105291,6306	4387,1408809	4387,1431560	109678,522023	109678,578899	-0,2295	-0,0918
6	106632,1518	106632,1505	3046,6219504	3046,6232675	109678,390214	109678,437630	-0,2914	-0,0971
7	107440,4413	107440,4405	2238,3324513	2238,3332810	109678,290114	109678,330769	-0,3149	-0,0900
8	107965,0517	107965,0511	1713,7220592	1713,7226151	109678,211786	109678,247368	-0,3202	-0,0801
9	108324,7225	108324,7221	1354,0512214	1354,0516120	109678,148936	109678,180570	-0,3165	-0,0703
10	108581,9928	108581,9925	1096,7809744	1096,7812592	109678,097442	109678,125916	-0,3083	-0,0617
11	108772,3435	108772,3433	906,4302025	906,4304165	109678,054506	109678,080394	-0,2981	-0,0542
12	108917,1208	108917,1207	761,6529040	761,6530688	109678,018175	109678,041907	-0,2870	-0,0478
13	109029,7916	109029,7914	648,9821718	648,9823015	109677,987041	109678,008948	-0,2759	-0,0424
14	109119,1923	109119,1922	559,5814289	559,5815327	109677,960068	109677,980411	-0,2649	-0,0378
15	109191,3163	109191,3162	487,4574955	487,4575799	109677,936478	109677,955466	-0,2544	-0,0339
16	109250,3444	109250,3443	428,4293581	428,4294276	109677,915674	109677,933476	-0,2445	-0,0306
17	109299,2655	109299,2654	379,5082948	379,5083528	109677,897191	109677,913948	-0,2350	-0,0277
18	109340,2618	109340,2617	338,5119774	338,5120262	109677,880663	109677,896489	-0,2262	-0,0251
19	109374,9569	109374,9569	303,8168028	303,8168443	109677,865795	109677,880789	-0,2178	-0,0229
20	109404,5791	109404,5791	274,1946309	274,1946665	109677,852350	109677,866592	-0,2100	-0,0210

a) series limit 109678,7737 cm^{-1}

b) ground state $-E_1=109678,773704$ cm^{-1}

c) similar data for np not shown but used for Fig. 2b and Fig. 2c

Table 2. For series $ns_{1/2}$: theoretical Rydberg fluctuations (26b) H PDW shifts and errors of Bohr theory. Precision test of polarization theory: data with and without fit, see (27b) (all data in cm^{-1})

n	$-E_{ns}$ [15]	ΔR (26b)(theo)	H PDW shifts (theo)	Errors ^{a)} Bohr theory	Errors ^{b)} (theo, no fit)	Errors ^{c)} (theo with fit)
1	109678,7737040	0,578405	0,001069	(0,00000)	(-0,001065)	(-0,003629)
2	27419,8178352	0,081759	0,124429	0,124410	-0,000018	-0,000109
3	12186,5502372	0,402917	0,019617	0,019826	0,000209	0,000010
4	6854,9188454	0,654754	-0,004705	-0,004511	0,000194	0,000013
5	4387,1408809	0,835058	-0,010223	-0,010067	0,000156	0,000008
6	3046,6219504	0,967428	-0,010777	-0,010652	0,000124	0,000005
7	2238,3324513	1,067938	-0,009969	-0,009869	0,000100	0,000003
8	1713,7220592	1,146580	-0,008861	-0,008780	0,000081	0,000002
9	1354,0512214	1,209677	-0,007780	-0,007713	0,000067	0,000001
10	1096,7809744	1,261372	-0,006819	-0,006763	0,000056	0,000000
11	906,4302025	1,304472	-0,005992	-0,005944	0,000048	0,000000
12	761,6529040	1,340942	-0,005288	-0,005247	0,000041	0,000000
13	648,9821718	1,372193	-0,004691	-0,004655	0,000036	0,000000
14	559,5814289	1,399267	-0,004183	-0,004151	0,000031	0,000000
15	487,4574955	1,422945	-0,003749	-0,003721	0,000028	0,000000
16	428,4293581	1,443826	-0,003376	-0,003352	0,000025	0,000000
17	379,5082948	1,462377	-0,003055	-0,003033	0,000022	0,000000
18	338,5119774	1,478966	-0,002776	-0,002756	0,000020	0,000000
19	303,8168028	1,493888	-0,002533	-0,002515	0,000018	0,000000
20	274,1946309	1,507382	-0,002320	-0,002303	0,000016	0,000000

a) Bohr theory, error for 19 levels 379,11 MHz

b) Polarization theory, error for 19 levels without fit 2,04 MHz, improvement by $380/2=190$

c) Polarization theory, error for 19 levels with fit 0,24 MHz, improvement by $380/0,25=1520$

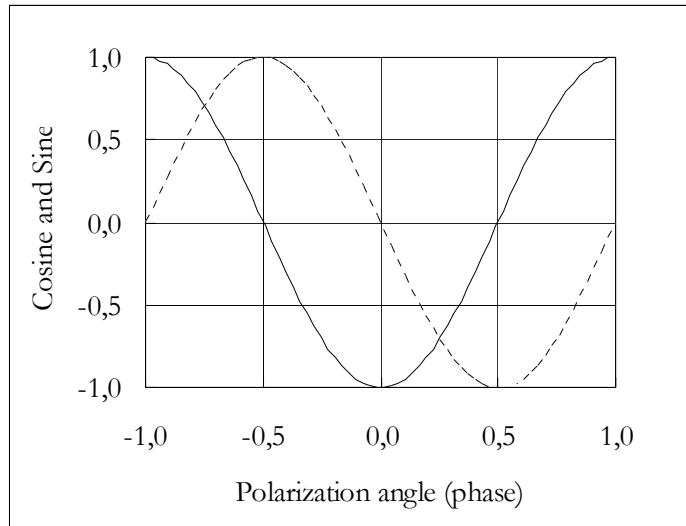


Fig. 1a Generic, system independent polarization: cos (full), sin (dashed)

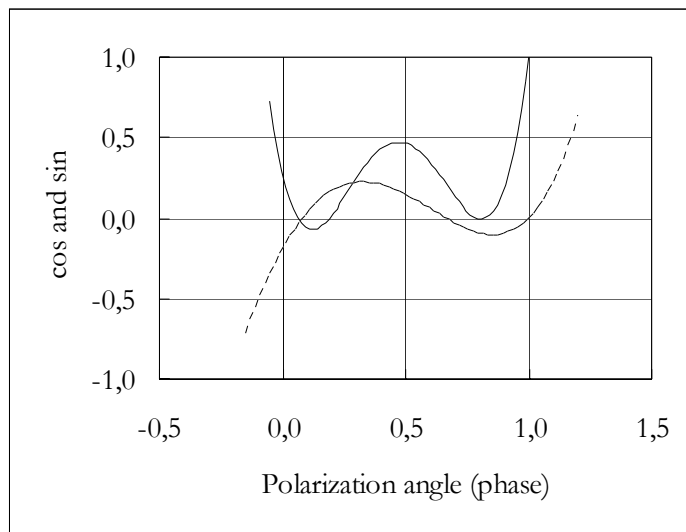


Fig. 1b Generic polarization attenuated by Bohr factor $1/n$: cos (full), sin (dashed)

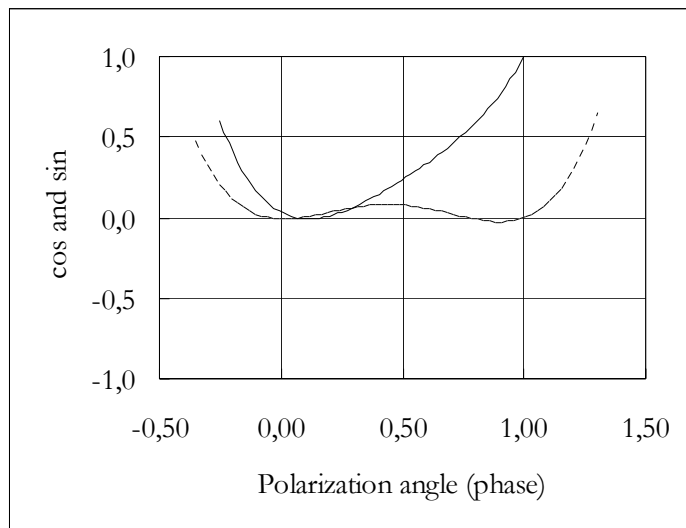


Fig. 1c Generic polarization attenuated by Bohr factor $1/n^2$: cos (full), sin (dashed)

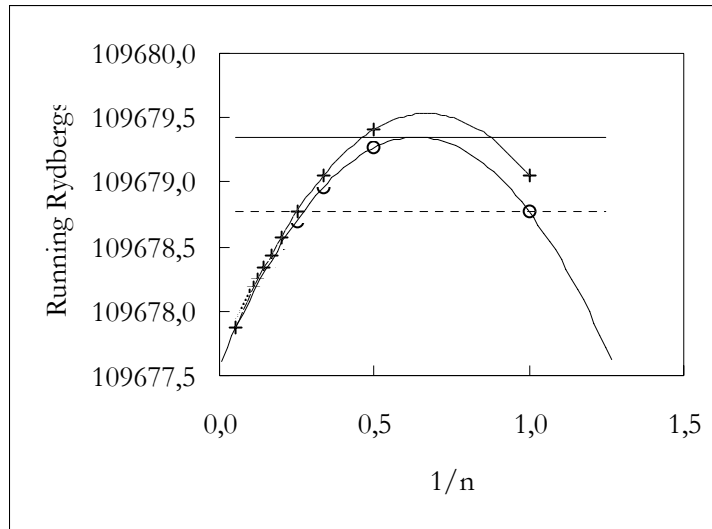


Fig. 2a Running Rydbergs curves: ns (full, extrapolated), np (dashed, not extrapolated), horizontal lines R_{harm} (full), ground state $-E_1=R_1$ (dashed)

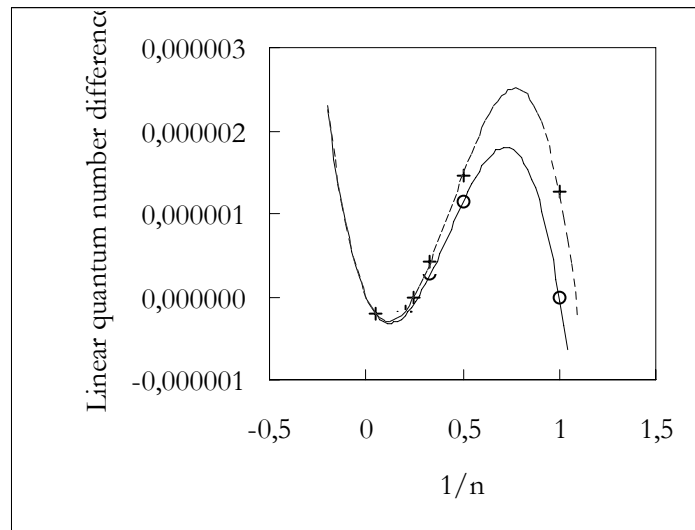


Fig. 2b Linear quantum number differences (5a): ns (full), np (dashed)

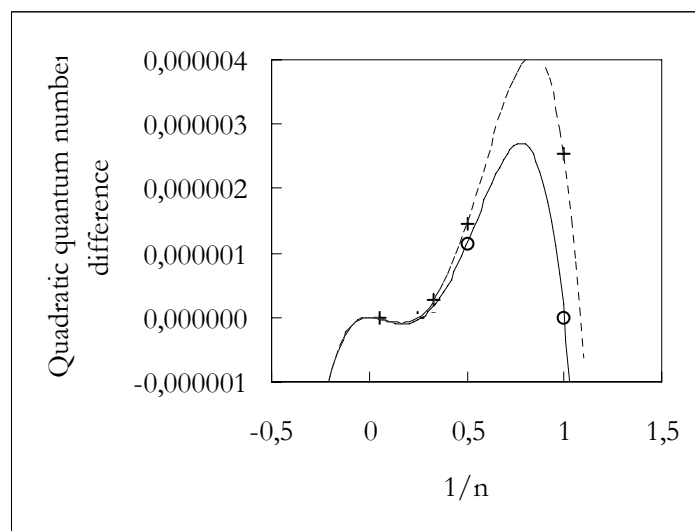


Fig. 2c Quadratic quantum number differences (5b): ns (full), np (dashed)

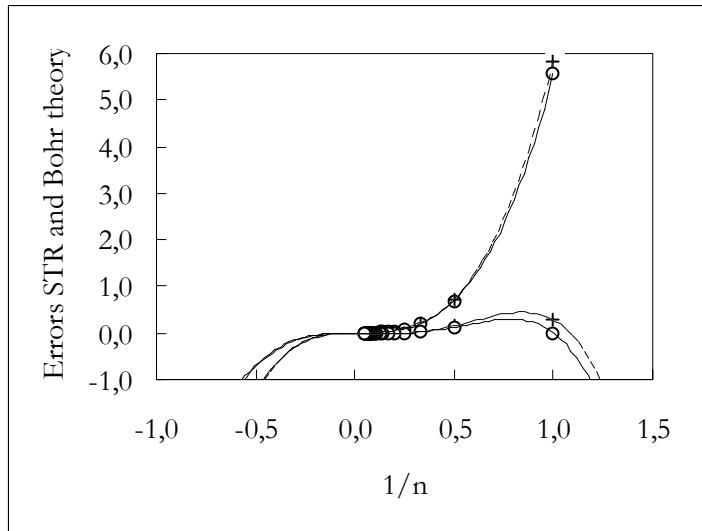


Fig. 2d Large repulsive errors (in cm^{-1}) with STR: upper right curves ns (o, full), np (+, dashed) and small sinusoidal errors with Bohr theory: lower right curves ns (o, full) and np (+, dashed)

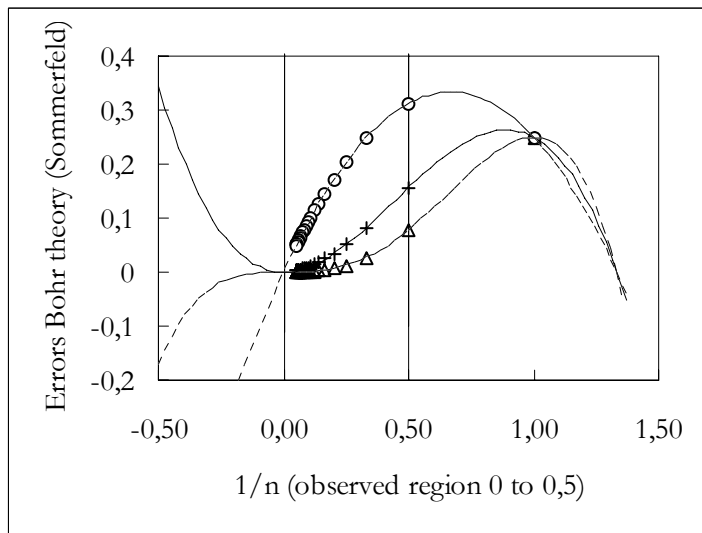


Fig. 3 Extrapolation beyond observed region: from parabola to cubic and to quartic

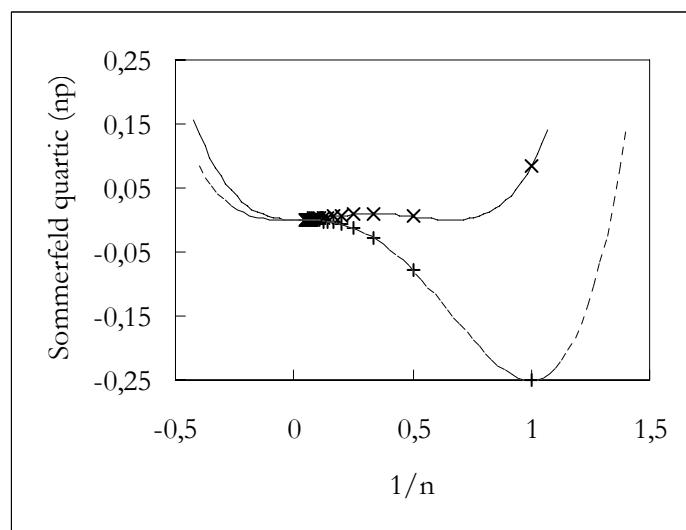


Fig. 4 Effect of asymptote shift on the shape of quartics: observed with ground state Rydberg (dashed) and theoretical with harmonic Rydberg (full)

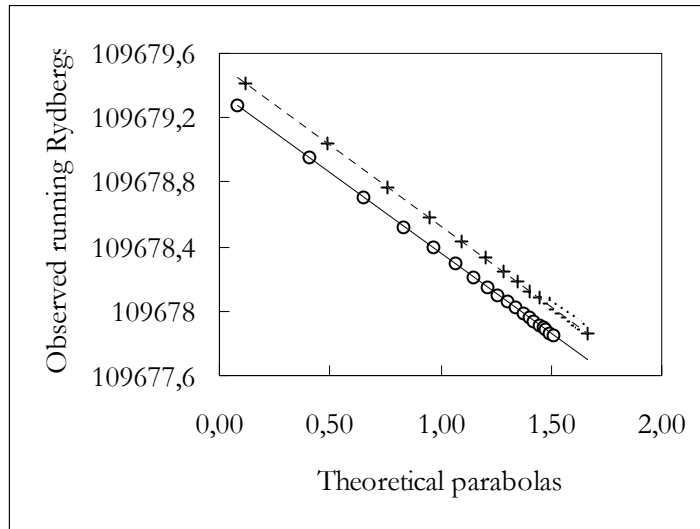


Fig. 5 Observed versus theoretical Rydberg differences:
 ns (o, full), fit $R_H(ns) = 109679,353174 - 0,995566\Delta R_{theo}$
 np (+, dashed) fit $R_H(np) = 109679,533968 - 1,001024\Delta R_{theo}$

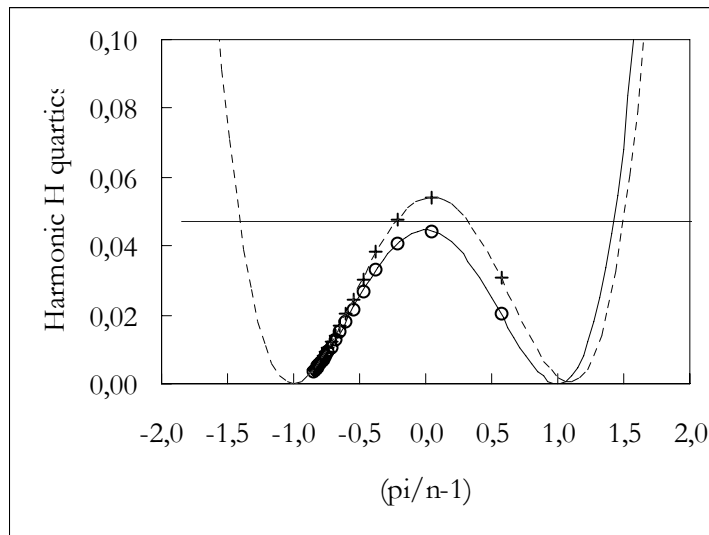


Fig. 6 H PDW shifts, the 21 cm line (horizontal) and harmonic H quartics: ns (o, full), np (+, dashed)

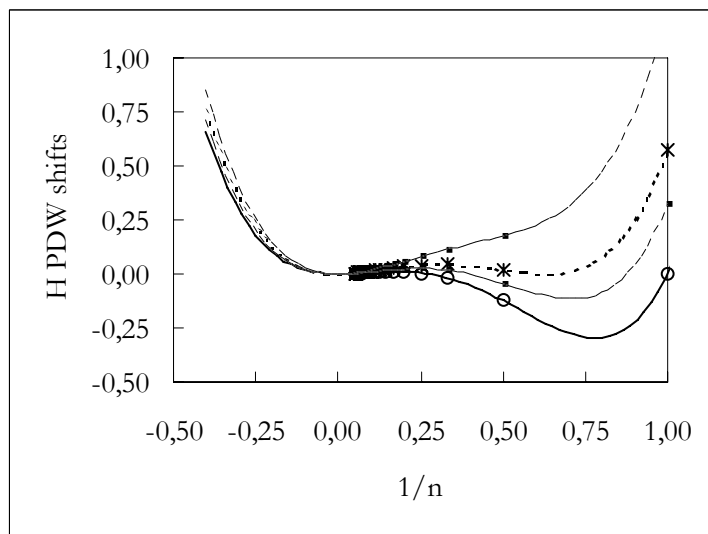


Fig. 7a. Mexican hat curves from HPDW shifts plotted versus $1/n$: bottom curve for ground state (o), intermediary (+, dashed), for harmonic R (*,dashed) as in Fig. 6, upper for large R (-, dashed)

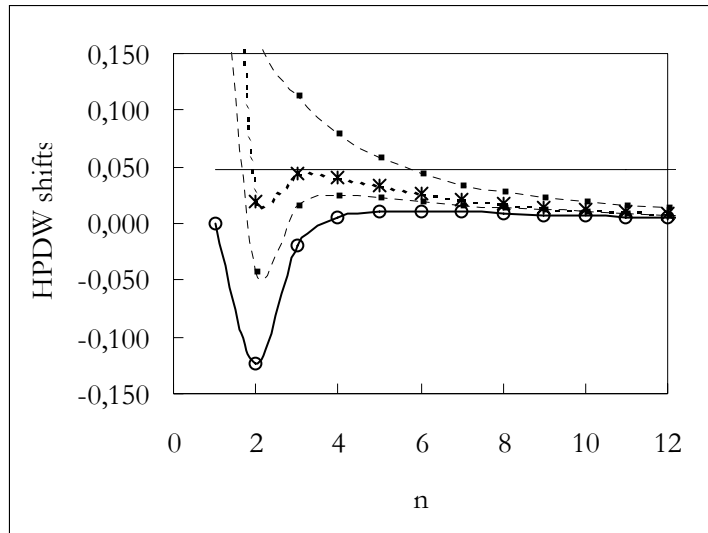


Fig. 7b. Van der Waals-Maxwell curves from HPDW shifts plotted versus n: bottom curve for ground state (o), intermediary (-, dashed), for harmonic R (*,dashed), upper for higher R (-, dashed). Full: 21 cm H line